Elsevier Editorial System(tm) for Journal of Chromatography A

Manuscript Draft

Manuscript Number: JCA-16-1434R1

Title: Pirkle-type chiral stationary phase on core-shell and fully porous particles: are superficially porous particles always the better choice towards ultrafast high-performance enantioseparations?

Article Type: Full length article

Keywords: Whelk-O1 superficially porous chiral stationary phase;
ultrafast enantioseparations;
mass transfer kinetics;
sub-second separation;
normal phase mode.

Corresponding Author: Prof. Alberto Cavazzini, PhD

Corresponding Author's Institution: University of Ferrara

First Author: Omar H Ismail

Order of Authors: Omar H Ismail; Luisa Pasti; Alessia Ciogli; Claudio Villani; Jelena Kocergin; Scott Anderson; Francesco Gasparrini; Alberto Cavazzini, PhD; Martina Catani

UNIVERSITY OF FERRARA
Department of Chemistry and Pharmaceutical Sciences

Via L. Borsari 46, 44121 Ferrara, Italy
Fax:+39-0532-240709

UNIVERSITÀ DEGLI STUDI DI FERRARA
- EX LABORE FRUCTUS -

Ref.: Revision MS JCA-16-1434

Dear Editor,

I am pleased to send you our response to reviewer comments on MS **JCA-16-1434**.

In this point-by-point response, for your convenience, our answers are reported in italic just after each comment of reviewers written in quotation marks.

At the end of the rebuttal letter, a copy of the paper where all changes made in the MS are clearly evidenced (in red: added text; strikeout: deleted text) has been included.

Thank you in advance for your time and cooperation.

With best regards,

Alberto Cavazzini
Francesco Gasparrini

Point-by-point response to reviewer comments

In this point-by-point response, line numbers indicating changes made to the MS refer to the revised version of the MS where changes are enlighten (in red: added text; strikeout: deleted text). This version is appended at the end of rebuttal letter.

Reviewer-1

"All what ref. 9 mentions about chiral SPS materials is "2.4. Selector immobilization on fused core HALO materials (subsection title) and the text "The HALO silica material was modified similarly to our previously published protocol [47]." Perhaps these authors even did not on purpose synthesize SPS-based CSP, did not study it and did not mention even single word about them in the entire discussion. Thus, when citing ref. 9 as very first work in this field the authors at least have to remark that this manuscript does not discuss these materials as such at all. The authors definitely understand who I am. Therefore, I do not have any problem to disclose my name to them. Fairness is the major issue in the scientific publishing and must be respected by everyone. Please avoid distributing wrong credits and give that to real pioneers. Since you by yourself have pioneered many interesting innovations in our common field of scientific interest following my concept above is very important for yourself."

This point was well taken. The reviewer is absolutely right. We apologize with him/her, as we also do believe that fairness is most important in science. The MS was accordingly changed (ll. 31-32). Hopefully, we have now given right credits to those who deserve it.

"Another example of wrong interpretation the literature is given in lines 50-51. I kindly ask the authors to carefully read ref. 10 in order to understand who for the first time recognized the advantage of SPS-based CSPs from the viewpoint of resolution per unit time discussed in these lines. Daniel Armstrong behaved unethical way declearing this as his own finding and the authors of the present manuscript propagate that wrong behavior. Prof. Gasparrini is very careful person and I am really very much surprised for his overlooking on this regard."

See our previous comment. Also in this case, the MS has been accordingly modified (ll. 34-38).

"Line 59 and elsewhere in the text: writing trans(italic)-stilbene oxide in this way seems to be better."

The advice was well taken and the text was modified.

"In the Experimental part the locations of USA companies must be cited according to the format "city, state, country" and the companies from other countries "city, country"."

The advice was well taken and locations were added in the Experimental part.

"In line 108 "Pirkle and co-workers" sounds better."

OK (see l. 116).

"Line 211 and elsewhere in the text. There are quite many passages written in personal style. Rewriting these to impersonal style is recommended."

The advice was well taken and, accordingly, the text was modified where needed.

"Ref. 12 is incorrect. It can be replaced with ref. 47."

The reviewer is right. Ref. 12 was corrected and ref. 47 was removed. Bibliographic references were accordingly updated

Reviewer-2

"Abstract, Line 6: Add µm after 2.6 in describing the SPPs."

The reviewer is right: "µm" was added after 2.6.

"Lines 13-17: I commend the authors for this statement as they have avoided the common argument of "lower RSD values" that many companies use as a key reason for good SPP performance in the A-term. While the hypothesis they discuss here may not necessarily be correct either (and clearly state as such), it tends to be in line with general observations and suggestions in a number of other recent publications."

Even though this point clearly needs additional experimental and theoretical work to be definitely answered, recent investigation is inclined to recognize particle roughness as one of the most important features.

"Lines 35-44: In terms of the discussion on the limited performance of chiral SPPs in capillary columns, this observation may not be limited to only chiral stationary phases but core-shell morphologies in general. In a 2015 paper on the comparison of 5 µm FPPs and SPPs in capillary columns (DOI: 10.3390/chromatography2030502), an exhaustive list of SPPs in capillary columns up to that point was provided (references 22-28 in said paper). It may not necessarily be the chiral phase that causes the issue, but rather differences in the wall effect (that has a bigger impact in capillary LC than it does in 1-4.6 mm bore columns) between SPPs and FPPs as performance also suffered in reversed phase C18 SPPs. Thus, in addition to the suggestion of difficulties of packing chiral phases mentioned here (Lines 42-43) it may be beneficial to note the overall difficulty in getting good SPP columns at the capillary scale. A more recent paper (DOI: 10.1016/j.chroma.2015.10.013) on packing
SPPs in capillaries at higher slurry concentrations gave the best reported efficiencies for such columns to date. This further supports potential reasoning as to wall effects playing a role in differences between SPPs and FPPs in capillaries as high slurry concentrations tend to reduce wall effects."

We thank the reviewer for this observation. The revised MS was modified to include these observations (see ll. 45-50). Bibliographic references suggested by the reviewer were added (new Refs. 13-19). Bibliography was accordingly updated.

"Lines 75-106: Between the article, the figure captions, and the supporting information, it is still not fully clear which LC was used for which section. I am led to believe that the Ultimate 3000 was used for most of the studies and that the Acquity was only used for the fast separations on the 1 cm column. Is this even correct?

Please add a statement clarifying what instrumentation was used for what data in both the section on 'van Deemter curve measurements' and in the relevant figure captions (Figure S2 is a good example that should be used elsewhere)."

We agree that this information was not clearly given. We apologize for that and we thank the reviewer for his/her careful reading of MS. The suggestion of the reviewer was accepted. In the revised MS (both in the experimental section, ll. 82 and 139-140, and in the figure captions) this information is now clearly given.

"Lines 110-116: As a key part of this manuscript is comparing different stationary phases that are coated with a chiral phase, the results of the coating process in terms of loadability should be described more in-depth for reader understanding. Please include information on how you calculated the values in Table 1 from the elemental analysis or cite a previous paper where such calculations are detailed. Also, more details on the column packing process should be provided to the reader or a previous citation from the group that describes their protocol should be included."

A detailed description on how values from elemental analysis were calculated could be found in ref. 30. Even though this reference was already present in the first version of the MS, we added a sentence to explain that readers can find there all the information to perform the calculations see l. 122).
More details on the packing process were also added (see ll. 125-129).

"Line 150: Please cite a source for the physical data related to the viscosity of THF."

Accordingly, ref. 35 was added.

"Line 175-177 (and 375-376): There is another recent Armstrong article not cited in this manuscript (DOI: 10.1016/j.chroma.2014.09.010) where the results in Table 1 (specifically the 3 um FPP and the 2.7 um SPP) do not follow this same trend. Do those different results based on a different CSP suggest one of the listed possible reasons for this difference in binding over another? Please address."

We thank the reviewer for this observation. We admit that we were not aware about that. The information is very important in the context of this work. Not only the reference to this paper was added to the MS, but the text of the paper was changed to account for this. (see ll. 186-190)

"Line 183: Remove 'relationship between'."

OK

"Line 193: The last part of this sentence ("the larger being the efficiency, the higher the resolution") should instead read something like "with higher efficiencies giving better resolution"."

The advice was well taken and the text was modified (see l. 214).

"Lines 214-221: This section is very confusing and needs to be rewritten. First, "in spite of the highest density of chiral selector" is true for one factor of bonding density, but the overall much larger surface area for FPPs can outweigh this factor. In that case, the alpha value differences for the FPPs would likely have a bigger difference than in the SPPs which would give higher resolution. Also, when comparing the FPPs, not only is it column length but also particle diameter that would play a role in the measured efficiency that would affect the calculated resolution."

We thank the reviewer for this observation. Indeed, he/she is correct. Accordingly, the discussion has been modified to include these points (ll. 239-243).

"Line 238: The data used to make the point about "less efficient packing" actually suggest "less dense packing" and the sentence should be changed to reflect that as packing density does not necessarily correlate with efficiency."

The advice was well taken and the text was modified (see ll. 263-265).

"Lines 265-267: Based on the flow rates at those given pressures, what would the expected power generated (W/m) be? Do those values exceed the Gritti/Guiochon standard value of 4 W/m for loss in efficiency due to radial temperature gradients?"

Yes, they do. For instance, at u_{int} = 0.8 and 1.0 cm/s, frictional power of respectively 20.2 and 30.9 W/m can be easily calculated.

"Line 289-291: The sentence regarding relating eddy dispersion and literature data is very confusing."

Thank you for reporting this. This part of the MS was modified (ll. 316-320). Hopefully now it is clearer.

“Lines 296-297: What is meant by "time needed for bed consolidation"? Time needed to fill the packed bed or time needed to flush at a higher pressure to compress the bed? Also, in the experimental section it was stated that the columns are packed up to 1000 bar. What pressure were the columns actually run at? For columns run with the Acquity, the pressure limit is 1000 bar, so columns packed at 1000 bar might not be stable there (as a higher packing pressure than what will be used for column use is required for stable beds).”

The time needed for bed consolidation in this paper is the time needed to compress the bed at high pressure flushing. This has been specified in the revised MS (ll. 325-326).

As for the comment about maximum pressure of packing vs. maximum operation pressure, there are not problems. Indeed, maximum pressures at which columns were operated are:

(i) long columns, 4 ml/min: 245 bar (2.6 µm SPP 150x4.6 mm), 460 bar (1.8 µm FPP 100x4.6 mm), 284 bar (2.5 µm FPP 150x4.6 mm) at 4 mL/min;

(ii) short columns, 8 ml/min: 260 bar (2.6 µm SPP 10x4.6 mm), 470 bar (1.8 µm FPP 10x4.6 mm) and 690 bar (1.8 µm FPP 10x3.0 mm).

“Lines 297-302: This is an extremely long sentence that needs to be broken into separate ideas or shortened. (Even if, undoubtedly, more investigation…, in particular…, the impression is…, i.e. ….).”

The advice was well taken and the sentence was shortened (see ll. 328-333).

“Line 335: Analysis time is decreased 30-50%, not gained.”

The reviewer is right. The text was modified (see l. 366).

“Lines 339-346 and Figure 4B: Figure 4B seems unnecessary as it just repeats data that is shown in Figure 4A and divides it. The numbers shown in 4B could easily be included in the caption for Figure 4 and then discussed in the text in the same way they already are with no information lost.”

It is true that Figure 4B does not introduce much more information that Figure 4a. In any case, in our opinion it visually gives a much clearer idea of the concept than a sentence written in the figure caption as this reviewer suggests. In addition, thinking about editorial issues, it is not an entire figure that should be removed but only a part of a figure. We decided accordingly to keep Figure 4 in its original form.

"Lines 347-364: The fast chiral separations demonstrated in this section (and Figure 5) are rather remarkable and one of the most interesting parts of the paper. As other work by the Armstrong group and others on high-speed chiral separations is already included throughout the articles, this might be a relevant spot to also mention recent results from the Belder group on these types of separations on microfluidic platforms (DOI: 10.1021/acs.analchem.5b00210). Also, all of these columns were 3-4.6 mm in diameter… Is there potential to reduce the diameter to 2.1 mm as a way to reduce the excessive flow rates that were used, especially if reductions in extra-column volumes can be made?"

First, we thank the reviewer for his/her nice comment. The advice to include a reference to the paper by Belder et al. was accepted (new reference 56). As for the observation about 2.1 diameter column, the answer is yes, in principle there is this possibility (in the sense that it is not a big issue to pack columns with this format). However, with 2.1 mm I.D. very short column, there is a big impact from extra volume contribution that, we fear, will dramatically impact on the separation. We are working on that and we hope to have soon some data to present.

"Line 397: 'possess' to 'possession'?"

The reviewer is right. The text was modified.

"In Figure S1, it says that the Acquity was modified to enable the use of 10 mm columns. However, in the text (Line 357) it says that the Dionex pump was employed. Please clarify what is the correct instrumentation used for these final studies (Figure 5 and Table 3)."

We thank the reviewer for this observation. A statement clarifying the instrumentation used was added in the captions of Figure 5 and Table 3.

"Figure caption clarifications: I would mention carbon tetrachloride as the dead time marker in the captions for Figures 1, 4, and 5 and TSO as the enantiomers that are being separated in the captions for Figures 4 and 5."

We thank the reviewer for this observation. Accordingly, captions of Figs. 1, 4 and 5 were modified.

"Reference 14 needs to be updated."

The reviewer is right. Ref. 14 was updated.

Pirkle-type chiral stationary phase on core-shell and fully porous particles: are superficially porous particles always the better choice towards ultrafast high-performance enantioseparations?

Omar H. Ismail[a], Luisa Pasti[b], Alessia Ciogli[a], Claudio Villani[a], Jelena Kocergin[c], Scott Anderson[c], Francesco Gasparrini[a,*], Alberto Cavazzini[b,**], Martina Catani[b]

[a]*Dept. of Drug Chemistry and Technology, "Sapienza" Università di Roma, P.le A. Moro 5, 00185 Roma, Italy*
[b]*Dept. of Chemistry and Pharmaceutical Sciences, University of Ferrara, via L. Borsari 46, 44121 Ferrara, Italy*
[c]*Regis Technologies, Inc., 8210 Austin Avenue, Morton Grove, IL 60053, USA*

Abstract

Pirkle-type Whelk-O1 chiral stationary phase (CSP) was prepared on 2.6 μm superficially porous particles (SPPs). The chromatographic behavior of columns packed with this new CSP was compared with that of columns packed respectively with 1.8 and 2.5 μm Whelk-O1 fully porous particles (FPPs). In the comparison, both thermodynamic and kinetic aspects were considered. Contrary to ~~our~~ initial expectations, chiral columns packed with 2.6 μm SPPs were quasi-comparable to those packed with 2.5 μm FPPs, apparently due to larger contributions to band broadening from both eddy dispersion and, especially for the second eluted enantiomer, adsorption-desorption kinetics. These findings raise the question if SPPs, in spite of the undeniable advantages of their morphology to speed up mass transfer, are always the best choice for high-efficient ultrafast chiral separations. The last part of the work focuses on the use of short columns (10 mm long) and very high flow rates to realize the separation of the enantiomers of *trans*-stilbene oxide (TSO) in normal phase mode in less than one second.

Keywords: Whelk-O1 superficially porous chiral stationary phase; ultrafast

*Corresponding author
**Corresponding author (phone:+39.0532.455331; fax: +39.0532.240709)
Email addresses: francesco.gasparrini@uniroma1.it (Francesco Gasparrini), cvz@unife.it (Alberto Cavazzini)

enantioseparations; mass transfer kinetics; sub-second separation; normal phase mode.

1. Introduction

Last generation superficially-porous particles (SPPs) [1, 2], referred to also as core-shell, fused-core or solid-core particles, are made of a non-porous fused silica core surrounded by a porous shell, whose volume is usually 60-75% of particle volume. In terms of mass transfer, core-shell structure offers some advantages over that of a fully porous particle (FPP) since the contributions to band broadening from both the longitudinal diffusion due to the relaxation of axial gradient concentration along the column (the so called B-term of the van Deemter equation) and the solid-liquid mass transfer resistance due to the diffusion across the particle (C-term of the van Deemter equation) are reduced by the presence of the inaccessible core. In addition, columns packed with C_{18}-SPPs have been demonstrated to be extremely efficient also thanks to the very low eddy diffusion, which comes from flow unevenness in the interstitial zone of the column (A-term of the van Deemter equation) [3–5]. Even though the explanation of the low A-term for columns packed with C_{18} SPPs remains to a large extent unknown, the most accepted hypothesis is that roughness of core-shell particles limits particle slipping after releasing the high pressure employed for the preparation of the packed bed by slurry-packing, therefore reducing radial bed heterogeneity [1, 2]. The reason of the great success of SPPs is that they have provided a reasonable compromise between two opposite tendencies. Indeed, the tendency to improve analytical throughputs by means of columns packed with smaller and smaller particles and reduced dimensions is limited by instrumental factors, such as the extremely high pressures needed to operate these columns at high flow rates, on the one hand, and the effect of system extra-column volume on peak broadening, on the other. As a matter of fact, columns packed with 2.7 μm SPPs are able to provide essentially the same efficiency as columns packed with sub 2-μm FPPs (keeping constant column dimensions and experimental conditions), but at operating pressures similar to those of columns packed with 3 μm FPPs [6, 7].

Surprisingly, the employment of SPPs in chiral chromatography is relatively recent [8]. The first work describing the use of SPPs in chiral HPLC dates 2011, when Lindner and coworkers prepared [9] a cinchona alkaloid based anion exchanger CSP by using 2.7 μm fused-core particles as base material~~,~~. The column was successfully employed for the enantioseparation of amide type amino acid derivatives~~.~~, even if the authors do not mention the possible advantages given by this typology of CSP. Chankvetadze and al. [10] firstly compared the kinetic performance of CSPs prepared on polysaccharide-coated FPPs and SPPs. They mentioned some of the benefits of chiral SPPs over their fully porous counterparts, such as an higher enantioselectivity at comparable content of chiral selector, a limited dependence of plate height on mobile phase flow rate and a larger enantioresolution per analysis time, with obvious benefits for high-throughput screening of chiral compounds [10]. By using 4.6 mm I.D.$\times$250 mm columns, they demonstrated that columns packed with SPPs outperform those packed with FPPs in terms of efficiency and speed of analysis. Fanali and coworkers [11, 12] employed the same polysaccharide-based chiral particles used in [10] to pack capillary columns (75μm I.D.$\times$25 cm) for nano-liquid chromatography and electrochromatography experiments. They report about the difficulty to efficiently operate these capillaries. They conclude that, without further optimization, this column format does not allow to reach useful efficiency for high-performance separation. Even if the authors do not discuss in detail the reason of the poor performance of these packed capillaries, more than on the kinetic performance of particles themselves, ~~in our opinion (see also later on in this paper)~~ this could depend~~s~~ either on the difficulty of efficiently packing chiral core-shell particles (and thus to the contribution of eddy dispersion to peak broadening) or on the overall difficulty in getting efficient SPP columns at the capillary scale~~, more than on the kinetic performance of particles themselves.~~ [13–19]

The most systematic work on the comparison between chiral FPPs and SPPs has been done by Armstrong's group [20–22]. With the aim of investigating the potential of chiral SPPs for ultrafast enantioseparations, Armstrong and coworkers characterized a wide variety of bonded brush-type CSPs prepared on 2.7 μm SPPs, including cyclofructan-6

based, β-cyclodextrin and macrocyclic antibiotics (in particular, teicoplanin, teicoplanin aglycone and vancomycin) [20]. ~~They first recognized that enantioresolution per analysis time significantly increases going from FPPs to SPPs [13,14], with obvious benefits for high-throughput screening of chiral compounds~~. The concept that emerges from these studies is that chiral SPPs outperform their FPP counterparts in any chromatographic mode, namely, reversed-phase (RP), normal phase (NP), polar organic and HILIC.

In the first part of this paper, we report about the synthesis of novel Pirkle-type Whelk-O1 2.6 μm chiral SPPs and the kinetic characterization of columns packed with these particles. To this scope, a comparison between the performance of these columns and those of columns packed with both 2.5 and 1.8 μm FPPs functionalized with identical chiral selector [23, 24] was performed by using *trans*-stilbene oxide (TSO) enantiomers as probes. In the second part of the work, the potential of Whelk-O1 CSPs for ultrafast enantioseparations on the second/sub-second time-scale is investigated by means of short columns (10 mm packed with both FFPs and SPPs) operated at very high flow rates (up to 8 ml/min).

2. Experimental section

Columns and materials. All solvents and reagents employed in this work were purchased from Sigma-Aldrich (St. Louis, MI, USA). Kromasil silica (1.8 and 2.5 μm particle size, 100 Å pore size, 323 m^2/g specific surface area) was from Akzo-Nobel (Bohus, Sweden). Whelk-O1 selector was generously donated by Regis Technologies Inc (Morton Grove, IL, USA). Accucore silica (2.6 μm particle size, 80 Å pore size, 130 m^2/g specific surface area, 0.5 μm shell thickness) was from Thermo Fisher Scientific (Waltham, MA, USA). 150 and 100 mm$\times$4.6 mm empty stainless steel columns were from IsoBar Systems by Idex (Erlangen, Germany), while 10$\times$4.6 and 10$\times$3.0 mm ones (including their holders) were fully developed and produced in-house. Fourteen polystyrene standards (from Supelco/Sigma-Aldrich, Milan, Italy) with molecular weights 500, 2000, 2500, 5000, 9000, 17500, 30000, 50000, 156000, 330000, 565000, 1030000, 1570000, 2310000 were employed for inverse size exclusion chromatography (ISEC).

Equipment. Two chromatographic equipments were employed in this work. Unless differently specified, ~~T~~the UHPLC chromatographic system used for 150 and 100 mm columns was an UltiMate 3000 RS system from Thermo Fisher Dionex (Whaltam, MA, USA) consisting of a dual gradient RS pump (flow rates up to 8.0 mL/min; pressure limit 800 bar under NP conditions), an in-line split loop Well Plate Sampler, a thermostated RS Column Ventilated Compartment and a diode array detector (UV Vanquish) with a low dispersion 2.5 μL flow cell. Detection wavelength was 214 nm (constant filter time: 0.002 s; data collection rate: 100 Hz; response time: 0.04 s). To reduce the extra-column contributions two 350$\times$0.10 mm I.D. Viper capillaries were used to connect the injector to the column and the column to the detector. The extra-column peak variance (calculated through peak moments) was 5.5 μL^2 in Hex/EtOH 90:10 + 1% MeOH at a flow-rate of 1.0 mL/min (extra-column volume: 12.2 μL). Data acquisition, data handling and instrument control were performed by Chromeleon (vers. 6.8) sofware.

An UPLC Acquity Waters system (Milford, MA, USA), equipped with a binary solvent manager (2mL/min maximum flow rate; pressure limit 1000 bar), an auto-sampler with a 5 μL injection loop, a thermostated column compartment (operated in still air conditions [5]), a diode array detector with a 500 nL flow cell, 80 Hz acquisition rate (resolution 4.8 nm; no filter time constant) was employed. Two Viper capillaries (250$\times$0.100 mm and 350$\times$0.100 mm $L\times$I.D.) were used as inlet and outlet connectors. The extra-column peak variance (through peak moments) was only 0.91 μL^2 at 1.0 mL/min. An updated version of Empower software was used in order to measure the second central time moments of the recorded concentration profiles. For the 10 mm columns, a modified version of the UPLC was used (Fig. S1 of Supplementary Data shows some images of the experimental arrangement). The programmable auto-sampler was replaced with an external in-house modified sample injector from VICI, Houston, TX, USA (model C74U). Essentially, this modification allowed for an electronic and fine control of the switching time (1.10 s) from injection to loading position and back. The injector is equipped with a 50 nL internal injection loop and a micro-electric actuator (Valco instruments, Houston, TX,

USA). The sample solution was introduced through a 25 μL syringe. This arrangement ensured consistent reduction of tailing effect and high reproducibility between injections. The standard inlet and outlet connecting tubes were replaced by two PEEK tubings of, respectively, 50 and 60 mm length $\times$ 63.5 μm I.D. With this configuration, the extra-column peak variance (through peak moments) was only 0.14 μL^2 at 1.0 mL/min.

Synthesis of Whelk-O1 SPPs and preparation of columns. Whelk-O1 SPPs were synthesized according to the procedure described by Pirkle and co-workers in 1992 [25, 26], which has been also employed for the synthesis of Whelk-O1 FPPs [27–29].

CHN elemental analysis for the different silica types functionalized in this work returned the following values: 6.28% C, 0.84% H and 0.73% N for 2.6 μm SPPs; 13.41% C, 1.73% H and 1.39% N for 1.8 μm FPPs; 13.30% C, 1.73% H and 1.38% N for 2.5 μm FPPs. Calculated bonding densities (based on N) are reported in Table 1. Details on how these calculations were performed can be found in reference [30]. FT-IR (KBr) of Whelk-O1 were: 2924, 2864, 1675, 1627, 1548, 1513, 1344, 1078 cm^{-1}.

All columns were slurry packed with a pneumatically driven Haskel pump (P_{max} = 1000 bar). The slurry solution (10% w/v of Whelk-O1 particles in acetone) was pushed into the column by using a mixture of hexane/2-propanol 90:10 (% v/v) as pushing solvent. The pressure was increased from 400 bar up to 1000 bar. 100 mL of pushing solvent were pumped into the column at 1000 bar to consolidate the bed. Decompression until atmospheric pressure was gradually performed.

van Deemter curve measurements. The kinetic performance of Whelk-O1 columns was evaluated in NP conditions. The mobile phase was a mixture of hexane/ethanol 90:10 (% v/v) + 1% methanol. Injection volumes were 0.1-0.5 μL. Temperature was set at 35°C. Retention time (t_R) and column efficiency (number of theoretical plates, N) of eluted peaks were automatically processed by the Chromeleon and Empower 3 software (using peak width at half height, according to European Pharmacopeia). N values were not corrected by extra-column contribution. The flow rates employed for studying the dependence of height equivalent to a theoretical plate H (=L/N, being L the column length) on the mo-

bile phase velocity started from 0.1 mL/min up to maximum respectively of 4.0 mL/min (for 100 and 150 mm long columns; equipment: Dionex 3000RS) and 2.0 ml/min (for 10 mm long columns; equipment: Waters Acquity), with constant steps of 0.1 mL/min. van Deemeter curves were plotted as H vs. interstitial velocity, u_{int}. u_{int} was calculated according to the well known equation:

$$u_{int} = \frac{F_v}{\pi r^2 \epsilon_e} \tag{1}$$

being F_v the flow rate, r the radius of the column and ϵ_e the interstial porosity. ϵ_e was calculated by ISEC experiments, as described below.

ISEC measurements, estimation of interstitial and total porosity and retention factor evaluation. ISEC measurements were performed by using tetrahydrofuran as mobile phase [31]. Injection volume, flow rate and detection wavelength were, respectively, 2 μL, 0.1 mL/min and 254 nm. For ISEC plots, retention volumes were corrected for the extra-column contribution before being plotted against the cubic root of the molecular weight (M_W). The interstitial volume, V_e, was derived from the extrapolation to $M_W = 0$ of the linear regression calculated for the volumes of the totally excluded polystyrene samples [32]. From this, the estimation of external column porosity, ϵ_e, is straightforward (being $\epsilon_e = V_e/V_{col}$, with V_{col} the geometric volume of the column). The ISEC estimation of the thermodynamic void volume, V_0, was based on the retention volume of benzene. Through this, the total porosity ϵ_t can be calculated ($\epsilon_t = V_0/V_{col}$).

The retention factor for the i-th enantiomer, k_i, was calculated by:

$$k_i = \frac{t_{R,i} - t_0}{t_0} \tag{2}$$

where $t_{R,i}$ is the retention time of the i-th enantiomer ($i = 1, 2$) and t_0 the void time calculated by using carbon tetrachloride (CCl_4) as marker.

Specific permeability and Kozeny-Carman constant. The specific permeability of each column was calculated according to the traditional equation [33, 34]:

$$k_0 = \frac{u\eta L}{\Delta P} \tag{3}$$

where $u = F_v/\pi r^2$ is the superficial velocity and η the viscosity of the eluent (0.46 cP for THF at 25°C [35]). ΔP is the difference between the total pressure drop, P_{tot}, and the system pressure drop (without the column), P_{ex}. P_{ex} was measured by replacing the column with a zero-volume connector. Experimentally, k_0 can be estimated by the slope of ΔP vs. u plot [36].

The Kozeny-Carman constant K_c was estimated by [33]:

$$K_c = \frac{\epsilon_e^3}{(1-\epsilon_e)^2}\frac{d_p^2}{k_0} \tag{4}$$

where d_p is the particle size (nominal d_ps given by manufacturer were used in this work in place of the more correct Sauter diameter value [5]).

3. Results and discussion

The preparation of SPPs was performed by following the same experimental protocol described in [27–29] for the functionalization of sub-2μm FPPs. The synthesis is particularly advantageous and reproducible even on SPPs, since phenomena such as particle aggregation and clogging or the non-uniform/excessive selector coating, frequently encountered with other chiral selectors, do not represent an issue with Whelk-O1 selector. Table 1 lists the characteristics of the particles employed in this work in terms of dimension, specific surface area, pore size (data from manufacturers) and chiral-selector loading (see Experimental section). Surface coverage is given both as μmol per gram of bare silica (column 6 of Table 1) and μmol per square meter (column 7). Several things can be observed from this table. The first is that the synthesis of FPPs of different dimensions is extremely reproducible (practically the same loading of chiral selector, about 390 μmol/g or 1.2 μmol/m^2, was found on the 1.8 and 2.5 μm FPPs). The second is that, by keeping constant the experimental conditions, functionalization of bare silica leads to significantly larger surface coverage of chiral selector (+ 20%) on SPPs (1.5 μmol/m^2) than on fully porous ones (1.2 μmol/m^2). This could be due to different reasons such as larger accessibility of external layers of particles, different surface chemistry of base silica FPPs and

SPPs, etc. However, it is difficult to generalize these findings. They are indeed consistent with previous reports by Armstrong and coworkers [20, 21], but contrast with other data from the same group [37]. ~~even though it is still uncertain why this happens (larger accessibility of external layers of particles, different surface chemistry of FPPs and SPPs, etc.).~~ Obviously, since the specific area per gram of FPPs is larger than that of SPPs, the total amount of chiral selector bounded per gram of base silica is also greater on the former type of particles than on fused-core ones. ~~This finding is consistent with previous reports by Armstrong and coworkers [13,14], even though it is still uncertain why this happens (larger accessibility of external layers of particles, different surface chemistry of FPPs and SPPs, etc.).~~

The common understanding is that the larger the amount of chiral-selector tethered to the surface, the larger the loadability of the phase (which is definitely important in preparative applications [38–40]) and the larger the retention factor. On the other hand, the relationship between enantioselectivity and surface coverage of chiral selector is not straightforward, since this last could impact also on the adsorption-desorption kinetics and thus on the separation efficiency. ~~relationship between~~ The resolution, R_s, of two chromatographic peaks (defined by the peak separation divided by the mean peak width) can be indeed expressed as [41]:

$$R_s = \frac{\sqrt{N}}{2}\frac{\alpha - 1}{\alpha + 1}\frac{\bar{k}}{1 + \bar{k}} \tag{5}$$

where N is the number of theoretical plates, and $\bar{k}$ and α are, respectively, the average retention factor (i.e., the average of retention factors of the two enantiomers) and the selectivity, defined by [42]:

$$\alpha = \frac{k_2}{k_1} \tag{6}$$

According to Eq. 5, one observes that resolution not only depends on the fact that solutes must be retained ($\bar{k} \neq 0$) and that they must be retained at different extent ($\alpha \neq 1$), but also on the efficiency of the column, ~~the larger being the efficiency, the higher the resolution~~ with higher efficiencies giving better resolution.

Fig. 1 shows the chromatograms recorded for the separation of TSO enantiomers on, respectively, the 150×4.6 mm I.D. column packed with 2.5 μm FPPs (top), the 100×4.6 mm I.D. one packed with 1.8 μm FPPs (middle) and, finally, the 150×4.6 mm I.D. column packed with 2.6 μm SPPs (bottom). On each column, the flow rate (see figure caption) at which the chromatogram was recorded corresponds to the optimal flow rate, that is where the van Deemter curve presents its minimum (see later on). For the sake of comparison between different columns, the x-axis is expressed as retention factor (in place of the traditional retention time). Retention factors were calculated by using CCl_4 as the void volume marker (see the experimental section). As it can be noticed from Fig. 1, on the two columns packed with 2.5 μm and 1.8 μm FPPs, TSO enantiomers are characterized by the same retention factors ($k_1 = 0.69$ and $k_2 = 1.72$), with α equal to 2.49. On the other hand, on the column packed with 2.6 μm SPPs, retention of both enantiomers is smaller ($k_1 = 0.50$ and $k_2 = 1.27$) but α is slightly larger (2.54). On the same figure the efficiency (N/m) of each peak has also been reported. N was calculated as described in the experimental section. In all cases, very large values were observed. In particular, on the 100×4.6 mm I.D. column packed with 1.8 μm FPPs (middle chromatogram), an efficiency as large as 292,000 and 271,000 N/m was obtained respectively for the first and the second eluted enantiomer. As a marginal remark, ~~we~~ it can be observed that these values are typical of efficient RP systems [5, 36]. The resolution of columns, estimated by eq. 5, resulted very large as well. R_s is 19.6 on the column packed with 1.8 μm FPPs, 20.2 for the column packed with 2.5 μm FPPs and 17.3 on the column packed with core-shell particles. Therefore, ~~in spite of the highest density of chiral-selector (see Table 1),~~ the column packed with SPPs has the lowest R_s, even if the surface density of chiral-selector measured on these particles was the highest (Table 1). However, the overall much higher surface area for FPPs can outweigh this feature and explain this fact. The difference in R_s between columns packed with FPPs ~~simply reflects~~ could reflect not only the difference in column length and thus in the total N per column (Fig. S2 of Supplementary Data graphically shows this concept by reporting, for the three columns, N per column as a function

of velocity) but also the impact of particle size (1.8 vs. 2.5 μm) on the measured efficiency. On the other hand, to explain the smallest R_s measured on the core-shell column one has to consider that the very favourable contribution of α is ruled out by both the effect of efficiency and retention.

Table 2 reports some of the physico-chemical parameters in use to assess the quality of column packing, at least from a qualitative viewpoint, such as the external porosity, ϵ_e, and the Kozeny-Carman constant (see Eq. 4). For well packed columns, ϵ_e is roughly 0.4 [1, 43] and 0.37 [5, 44] respectively for beds made of core-shell and fully porous particles and the K_c constant is close to 180 [33]. As it can be seen from this table, for all columns ϵ_e was about 40%. However, while the columns packed with FPPs have K_c equal to 180, for the one packed with SPPs K_c is only 160. For the sake of completeness, in Table 2, the total porosities, ϵ_t, of columns are also reported (see the experimental section for details). Their values are close to typical values for columns packed with fully porous (0.65-0.7) and core-shell (0.52-0.55) particles [32, 39, 45].

The other important information that can be derived from Table 2 is about the permeability (see Eq. 3) of columns. As expected, the column packed with 1.8 μm FPPs is characterized by the smallest k_0 value, 2.95×10^{-11} cm^2, which reflects the difficulty of delivering a flow in a bed made of very fine particles. Surprisingly, the column packed with 2.6 SPPs results to be about 25% more permeable than that packed with 2.5 FPPs, even tough their ϵ_e are very similar. ~~Together with the already discussed low value of K_c, this could suggest a less efficient packing of SPPs (see later on).~~ This could suggest a less dense packing of SPPs that, together with the already discussed low value of K_c, could affect the kinetic performance of the column.

When the van Deemter equation is employed in chiral chromatography, in addition to the traditional terms describing longitudinal diffusion (B), eddy dispersion (A) and solid-liquid mass transfer kinetics (C_S), an additional term taking into account the slow adsorption-desorption kinetics (C_{ads}), which frequently characterizes enantiorecognition phenomena, is also added [4, 46]. The dependence of H on the mobile phase velocity is

therefore written as:

$$H = A(u) + \frac{B}{u} + C_S u + C_{ads} u \tag{7}$$

Fig. 2 shows the van Deemter curves of TSO enantiomers measured, respectively, on the 150×4.6 mm column packed with 2.5 μm FPPs (top), on the 150×4.6 mm one packed with 2.6 μm SPPs (middle) and on the 100×4.6 mm column packed with 1.8 μm FPPs (bottom). Diamonds (green) refer to the first enantiomer and circles (blue) to the second one. The height equivalent to a theoretical plate has been plotted against the interstitial velocity, u_{int} (Eq. 1), which represents the true linear velocity of the mobile phase (since the fluid flows around and between the particles, not through them). These plots suggest some considerations. First, one may observe that the longitudinal diffusion of the two enantiomers in each column is the same. This is demonstrated by the overlapping of their van Deemter curves at low flow rates (where the *B*-term is dominant). Then, under the assumption of the same eddy dispersion for the two enantiomers in a given column [47], the conclusion is reached that the difference in the van Deemter curves (already evident at relatively low linear velocity, starting at u_{int} roughly 0.3 cm/s) is essentially due to a slow adsorption-desorption process. This is particularly evident for the column packed with 2.6 μm SPPs (middle plot). Another interesting observation coming from Fig. 2 is that the slope of the *C*-branch of the van Deemter equation is markedly steeper for the column packed with 1.8 μm FPPs (bottom part of the figure) than for columns packed with both 2.5μm FPPs (top) and 2.6 μm SPPs (middle). This is due to frictional heating generated by the stream of mobile phase against the packed bed of the column through which it percolates under significant pressure gradient [48–50]. For instance, at u_{int}=0.8 cm/s, the back-pressure generated by the 1.8 μm column was 5300 psi and, at u_{int}=1.0 cm/s, it reached 6750 psi. The heat produced locally is dissipated in both the radial and longitudinal direction of the column. This generates longitudinal and radial temperature gradients, whose amplitude depends on the degree of thermal insulation of the column (either adiabatic or isothermal). The column compartment of the Dionex UHPLC equipment used for the measurement of the van Deemter curves with these columns (see Experimental section)

can only work in the so-called forced-air mode (quasi-isothermal conditions), where it is well known that radial temperature gradients degrade the efficiency of column [51–53].

With the purpose of comparing the behavior of the three columns, in Fig. 3 van Deemter curves of the first and the second TSO enantiomer are overlapped. Curves on top of this figure are those for the less retained enantiomer, while on the bottom there are the van Deemter curves relative to the second enantiomer. The kinetic behavior of the first enantiomer looks very similar on all columns, in consequence of the very low retention (see Fig. 1) of this compound that does not allow to draw any significant conclusion on mass transfer phenomena. The only minor difference is around the minimum of van Deemter curves, where the core-shell column is the less efficient (see later on).

By considering the second enantiomer (bottom part of Fig. 3), very different kinetic behaviors can be observed, depending on column. Unexpectedly, the column packed with Whelk-O1 2.6 μm SPPs (circles, purple), no matter the flow rate, is characterized by the worst performance, even worse than its 2.5 μm fully porous counterpart (diamonds, cyan). This is a surprising result that contrasts with the commonly observed performance of columns packed with C_{18} SPPs [6, 7]. It can be explained by considering the contribution to band broadening coming from either eddy dispersion or slow adsorption-desorption kinetics or a combination of both. The first statement, about the importance of eddy dispersion in columns packed with SPPs~~is not supported by literature data, as it was mentioned before~~, is counter intuitive at least according to literature data that demonstrate how packed beds made of SPPs are expected to be more efficient than those of FPPs (see before). It ~~is~~ can be however suggested by the experimental difficulties encountered during the slurry packing of Whelk-O1 SPPs. By considering their characteristics, first of all that these particles are polar, however it does not seem weird that they behave differently from hydrophobic C_{18} ones during the slurry packing [19, 54]. As a matter of fact, not only the achievement of stable slurry suspensions was more difficult with very polar SPPs than with Whelk-O1 fully porous ones but also, e.g., the time needed to compress the bed (by high-pressure flushing) ~~for bed consolidation~~ did not follow any expected

trend and could not be optimized. ~~Even if, undoubtedly, more investigation is needed in this field, in particular on the rheological characteristics of Whelk-O1 SPPs,~~In conclusion, the impression is that one of the most important characteristics of hydrophobic core-shell particles, i.e. their ability to generate very efficient packed beds ~~characterized by very low eddy dispersion~~, could not be easily reproducible with very polar Whelk-O1 SPPs. Further investigation is needed to assess this point, in particular on rheological characteristics of Whelk-O1 SPPs. In agreement with [11, 12], ~~we may~~ it should be concluded ~~this reasoning by saying~~ that the efficient preparation of packed beds of polar SPPs still requires a long way to go. This essentially needs the optimization of all steps of packing protocol, without which the full potential of polar chiral SPPs can be barely reached.

As mentioned before, on the 2.6 μm Whelk-O1 core-shell column the contribution to band broadening coming from a slow mass transfer process seems to be particularly evident. Since the solid-liquid mass transfer term (C_s) should be lower on core-shell than on fully porous particles (due to the presence of the inaccessible core), the conclusion is that the adsorption-desorption kinetics must be slower on core-shell particles (higher C_{ads} term in eq. 7) than on the fully porous ones. An explanation could be the different surface density of chiral selector between core-shell and FPPs. Table 1 shows that this surface density is about 20% larger on SPPs than on fully porous ones. In literature there are practically no studies which have attempted to assess if and how chiral recognition is modified by changing the amount of chiral selector tethered to the surface and how this could impact on the chromatographic performance [12]. On the other hand, ~~we believe~~ this is a very important subject that needs more experimental and theoretical work to be fully understood.

Finally, by still looking at the bottom part of Fig. 3, it is evident that the column packed with 1.8 μm FPPs (triangles, green) outperform the other two in terms of kinetic behavior but it is also clear that, at high flow rates, where the effect of frictional heating on efficiency is dominant, this column does not offer any advantage over the one packed with 2.5 μm FPPs. Indeed, at u_{int} slightly larger than 1 cm/s, the *C*-branch of the 1.8 μm

fully porous column merges to that of the column packed with 2.5 μm FPPs.

Fig. 4 (top) shows the gain in analysis time that can be obtained by moving from both the columns packed with 2.5 μm FPPs and 2.6 μm SPPs to that packed with 1.8 μm FPPs. The necessary premise to discuss this figure – whose meaning~~, we want to point out,~~ is merely practical – is that the length of commercially available columns packed with 2.5-2.7 μm particles (no matter if fully porous or pellicular) is usually 150 mm, while that of columns packed with sub-2μm particles is only 100 mm or less. This justifies the direct comparison presented in Fig. 4, where column length is not accounted for. Having acknowledged this, and by referring for each column to condition of maximum efficiency (indeed chromatograms presented in Fig. 4 were recorded at the optimum flow rate, see figure caption for details), one observes that the column packed with 1.8 μm FPPs permits to ~~gain~~ decrease analysis time more than 50 and 30% ~~of analysis time~~ (here simply calculated as the retention time of the second eluted enantiomer) with respect to, respectively, the 2.5 μm fully porous column and the 2.6 μm core-shell one. The practical advantage achievable with the 100 mm column packed with sub-2μm particles, becomes still more evident by considering, in addition to analysis time, also the resolution of columns (see before). Thus, the ratio between resolution and analysis time [55], graphically given as bar chart in the bottom part of Fig. 4, is strongly favorable for the 1.8 μm column packed with FPPs (it is indeed 11.9 on this column vs. 5.3 and 7.9 on, respectively, the 2.5 μm fully porous and the 2.6 μm core-shell column). Incidentally, the gain of $R_s/t_{R,2}$ ratio observed for the 2.6 μm core-shell column over that packed with 2.5 μm FPPs comes from the reduction of retention time in the former column (due to a much lower total surface area per column) and not from an increase of R_s (which actually is larger on the 2.5 μm fully porous column).

The last part of this study briefly reports on the use of short columns, packed with both Whelk-O1 FPPs and SPPs, to realize ultrafast enantioseparations. In this proof-of-concept study, 10 mm columns of different I.D. (3.0 and 4.6 mm) were employed. These columns were in-house designed and developed. Fig. S3 of Supplementary Data shows a picture

of the 10 mm column and holder. They were packed by following the same protocol also used for longer columns. Table 3 has some information that helps to characterize these columns, in particular the optimal flow rate (i.e., the flow rate corresponding to the minimum of van Deemter curve), the corresponding interstitial linear velocity and the maximum efficiency (in N/m). With the purpose of performing ultrafast enantioseparations, these columns were operated at the maximum flow achievable by ~~our~~ instrumentation (8 ml/min). Accordingly, the Thermo Dionex equipment (see experimental section) was employed, even though its extra-column variance is not negligible with respect to that of first and second eluted enantiomers (respectively, roughly 11.2 and 28 $\mu\mathrm{L}^2$). In the last column of Table 3, the number of theoretical plates per column measured at the highest flow rate is reported. As an example, Fig. 5 shows the chromatogram recorded with the 10×3.0 mm column packed with 1.8 μm FPPs. As it can be seen, the separation of TSO enantiomers was performed in less than 1 s, with $R_s = 2.2$. This represents an extraordinary result, unimaginable only a few years ago in chiral liquid chromatography, which is even comparable with that of chiral separations on microchip platforms [56].

4. Conclusions

The investigation of the kinetic performance of columns packed with Whelk-O1 fully porous and core-shell particles of similar diameter (2.5 μm for FPPs vs. 2.6 μm for core-shell ones) has surprisingly revealed that FPPs outperform SPPs. This depends, in part, on the faster mass-transfer adsorption-desorption kinetics observed (especially on the second eluted enantiomer) on the FPPs and, in part, on the smaller eddy dispersion contribution to band broadening on the column packed with FPPs. The slower mass-transfer adsorption-desorption process is most likely due to the larger surface density of chiral selector on the SPPs. Indeed, even though the same experimental conditions were maintained during functionalization of SPPs and FPPs, the outcome was different. The surface density of Whelk-O1 selector on SPPs was indeed 20% larger than that of FPPs. ~~This finding is consistent with previous results from Armstrong et al. [13,14] and seems to be a~~

~~characteristic feature in the derivatization of core-shell particles.~~ ~~Our~~ These results suggest that, at least for the case considered in this work, the higher the surface coverage, the lower the adsorption-desorption process but with the information in our possession no generalization can be made. Fundamental studies aimed at investigating the relationship between mass transfer kinetics and surface density of chiral selector are needed.

On the other hand, the empirical difficulty to pack Whelk-O1 core-shell particles explains the important eddy dispersion contribution to band broadening in columns packed with these particles. Different attempts have been done to improve the packing process, by varying many experimental variables (slurry composition, consolidation time, etc.) during the packing, but without success. These findings show that packing polar SPPs is significantly different from packing hydrophobic SPPs (such as C_{18} particles), for which a large amount of information and expertise has been collected over the years. One of the most significant characteristics of beds made of C_{18} core-shell particles is their extremely low eddy dispersion term. This, however, seems to be difficult to achieve with Whelk-O1 SPPs. The investigation of rheological properties of these particles can help to understand their different behavior with respect to fully porous particles so to optimize the packing protocol and, thus, the kinetic performance of columns made of polar Whelk-O1 SPPs.

5. Acknowledgments

The authors thank the Italian University and Scientific Research Ministry (Grant PRIN 2012ATMNJ_003) and the Laboratory Terra&Acqua Tech, member of Energy and Environment Cluster, Technopole of Ferrara of Emilia-Romagna High Technology Network. Dr. Valentina Costa from the University of Ferrara is acknowledged for technical support. The authors thank Thermo Fisher for providing Accucore 2.6 μm SPP silica.

Appendix A. Supplementary Data

Supplementary data associated with this article can be found in the online version.

6. Figures and Tables

Figure captions

Fig 1. Chromatograms showing the separation of TSO enantiomers on the three columns employed in this work. Carbon tetrachloride was used as dead time marker. Top: 150×4.6 mm column packed with Whelk-O1 2.5 μm FPPs; middle: 100×4.6 mm column packed with Whelk-O1 1.8 μm FPPs; bottom: 150×4.6 mm column packed with Whelk-O1 2.6 μm SPPs. Chromatograms were recorded at the flow rate corresponding to the minimum of the van Deemter curve (they were, from top to bottom, respectively 1.2, 1.8 and 1.5 ml/min). For the sake of comparison, x-axis is given in terms of retention factor instead of retention time. Close to each peak, efficiency (N/m), retention factor (k) and retention time (t_R) are indicated. Instrument employed for measurements: UPLC Waters Acquity.

Fig 2. van Deemter curves for TSO enantiomers measured on Whelk-O1 columns (same geometries as in Fig. 1) packed with, respectively, 2.5 μm FPPs (top), 2.6 μm SPPs (middle) and 1.8 μm FPPs (bottom). Instrument employed for measurements: Dionex 3000RS.

Fig 3. Overlapped van Deemter curves measured on the three Whelk-O1 columns (same geometries as in Fig. 1), respectively for the first (top) and the secondly (bottom) eluted TSO enantiomers. Diamonds: column packed with 2.5 μm FPPs; circles: column packed with 2.6 μm SPPs; triangles: column packed with 1.8 μm FPPs. Instrument employed for measurements: Dionex 3000RS. See text for details.

Fig 4. A) Same chromatograms as in Fig. 1, showing the separation of TSO enantiomers on the three columns employed in this work, but with the x-axis given in retention time. Carbon tetrachloride was used as dead time marker. B) Bar chart showing the ratio between resolution and retention time for the 2.6 μm core-shell column (first bar on the left, blue color), the 1.8 μm fully porous column (middle bar, orange) and, finally, the 2.5 μm

fully porous column (last bar on the right, red). Ratios were calculated on the second eluted enantiomer. Instrument employed for measurements: UPLC Waters Acquity.

Fig 5. Example of ultrafast enantioseparation thanks to the use of short column and high flow rate. In this particular case, a 10×3.0 mm column packed with 1.8 μm FPPs was operated at 8 ml/min (u_{int} = 4.8 cm/s) for the separation of TSO enantiomers. Carbon tetrachloride was used as dead time marker. Note the time scale in seconds. Instrument employed for measurements: Dionex 3000RS. See text for details.

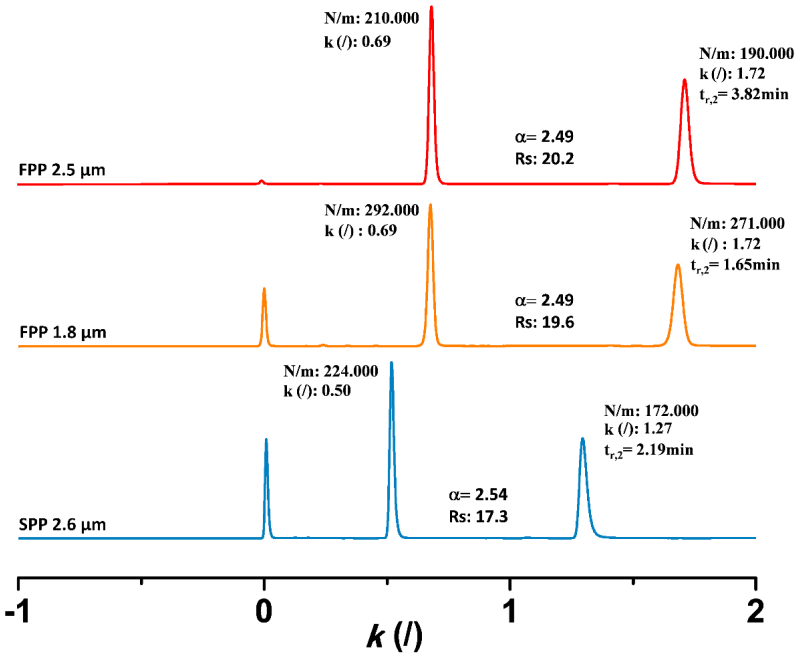

Figure 1:

Figure 1:

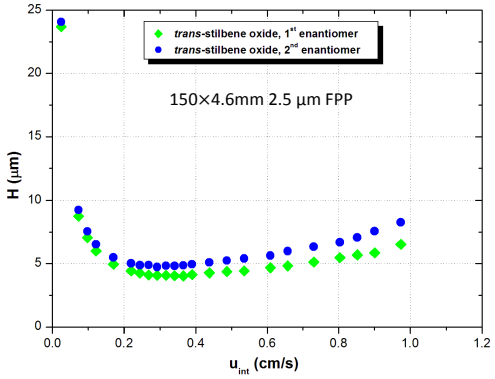
trans-stilbene oxide, 1st enantiomer
trans-stilbene oxide, 2nd enantiomer
150×4.6mm 2.5 µm FPP
H (µm)
u_int (cm/s)

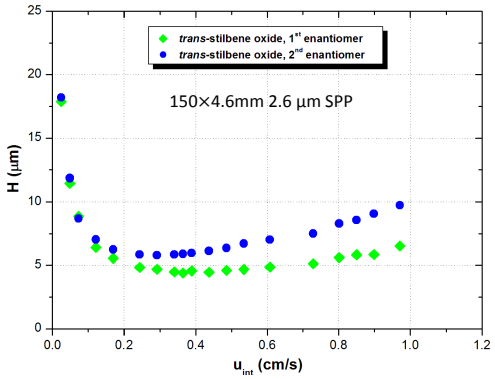
trans-stilbene oxide, 1st enantiomer
trans-stilbene oxide, 2nd enantiomer
150×4.6mm 2.6 µm SPP
H (µm)
u_int (cm/s)

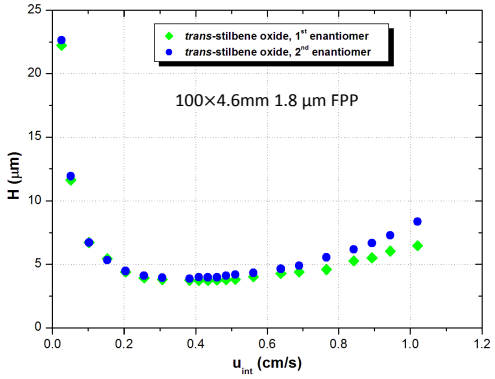
trans-stilbene oxide, 1st enantiomer
trans-stilbene oxide, 2nd enantiomer
100×4.6mm 1.8 µm FPP
H (µm)
u_int (cm/s)

Figure 2:

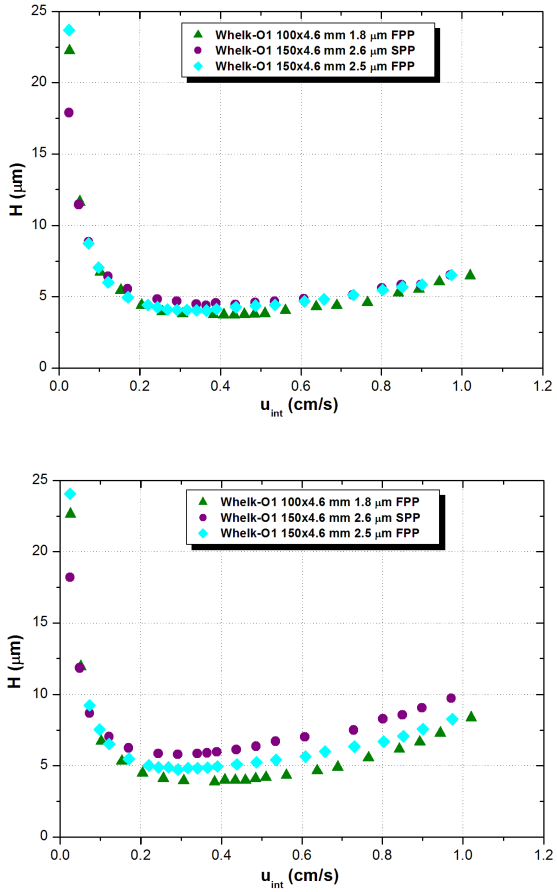
Whelk-O1 100x4.6 mm 1.8 µm FPP
Whelk-O1 150x4.6 mm 2.6 µm SPP
Whelk-O1 150x4.6 mm 2.5 µm FPP
H (µm)
u_int (cm/s)
0
5
10
15
20
25
0.0
0.2
0.4
0.6
0.8
1.0
1.2

Figure 3:

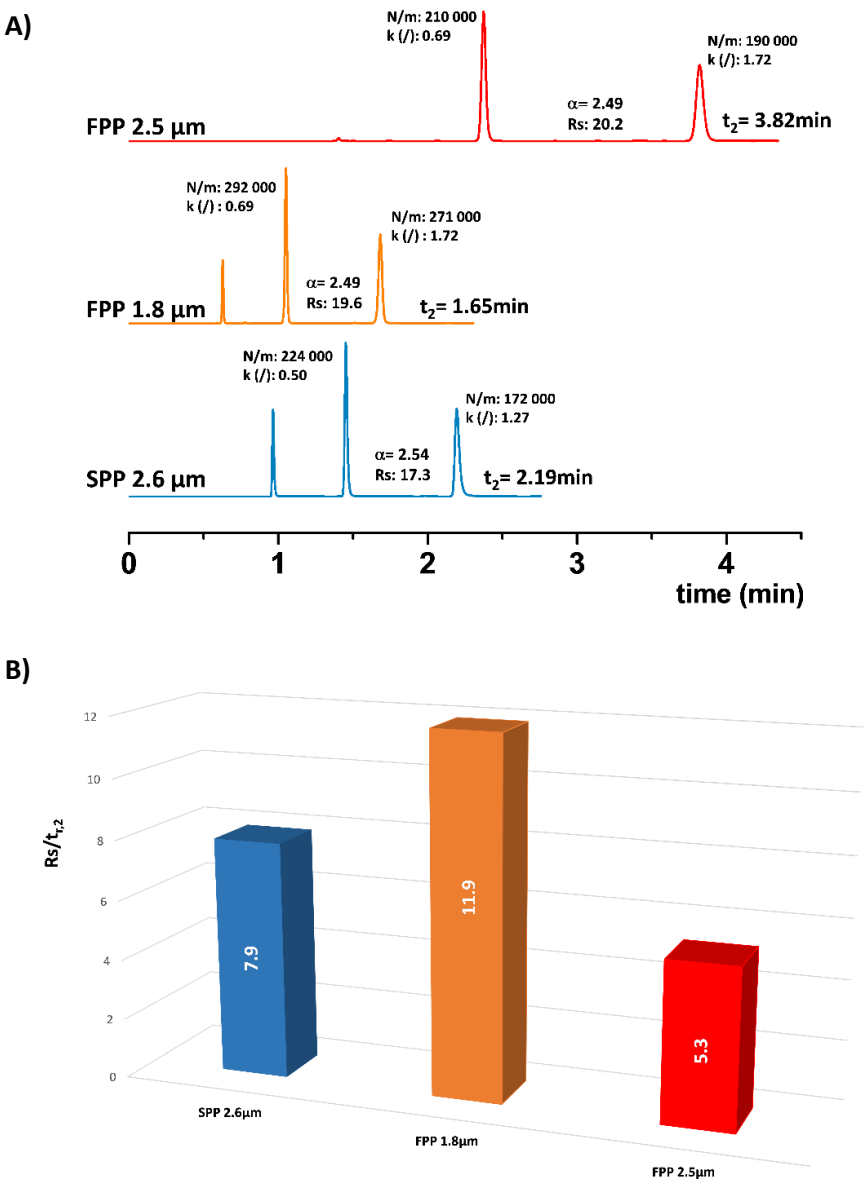
A)
N/m: 210 000
k (/): 0.69
N/m: 190 000
k (/): 1.72
α= 2.49
Rs: 20.2
FPP 2.5 µm
t2= 3.82min
N/m: 292 000
k (/) : 0.69
N/m: 271 000
k (/) : 1.72
α= 2.49
Rs: 19.6
FPP 1.8 µm
t2= 1.65min
N/m: 224 000
k (/): 0.50
N/m: 172 000
k (/): 1.27
α= 2.54
Rs: 17.3
SPP 2.6 µm
t2= 2.19min
0
1
2
3
4
time (min)
B)
Rs/t1,2
12
10
8
6
4
2
0
7.9
11.9
5.3
SPP 2.6µm
FPP 1.8µm
FPP 2.5µm

Figure 4:

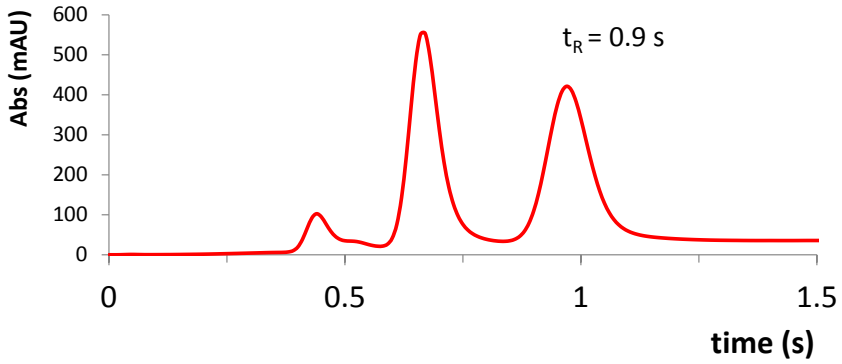

Figure 5:

Table 1: Geometrical characteristics of Whelk-O1 columns: particle type (FP: fully porous, SP: superficially porous); column dimensions; particle diameter (d_p); specific surface area (A_s); pore size; bonding density (given both as μmol per gram of bare silica and μmol per square meter).

Particle type	Dimensions	d_p	A_s	Pore size	Bonding density	
	(L×I.D., mm)	(μm)	(m^2/g)	(Å)	(μmol/g)	(μmol/m^2)
FP	150×4.6	2.5	323	100	391.2	1.21
FP	100×4.6	1.8	323	100	394.6	1.22
SP	150×4.6	2.6	130	80	189.8	1.46

Table 2: Physico-chemical properties of Whelk-O1 columns: particle type (FP: fully porous, SP: superficially porous); total porosity (ϵ_t); external porosity (ϵ_e); Kozeny-Carman constant (K_c); permeability (k_0).

Particle type	ϵ_t	ϵ_e	K_c	$k_0 \times 10^{11}$ (cm^2)
FP	0.670	0.412	180	7.06
FP	0.644	0.393	180	2.95
SP	0.524	0.413	160	8.60

Table 3: Kinetic performance (in N/m) of short columns (10 mm) of different diameter. $F_{v,opt}$ and $u_{int,opt}$ represent, respectively, the optimum flow rate (that is the flow rate corresponding to the minimum of the van Deemter curve) and the optimum interstial velocity; N_{max} is the number of theoretical plates per column, when the column was operated at 8 ml/min (see text for more details). In all cases, N has been calculated as the average value of Ns of the two TSO enantiomers. Particle type: FP, fully porous; SP, superficially porous). Instruments employed for measurements: UPLC Waters Acquity for van Deemter curves; Dionex 3000RS for ultrafast enantioseparations (evaluation of N_{max}).

Particle type	L×I.D. (mm)	$F_{v,opt}$ (mL/min)	$u_{int,opt}$ (cm/s)	N/m	N_{max}
FP	10×4.6	1.7	0.43	190,000	1220
SP	10×4.6	1.5	0.36	140,000	850
FP	10×3.0	0.7	0.42	180,000	520

References

[1] G. Guiochon, F. Gritti, Shell particles, trials, tribulations and triumphs, J. Chromatogr. A 1218 (2011) 1915–1938.

[2] R. Hayes, A. Ahmed, T. Edge, H. Zhang, Core-shell particles: preparation, fundamentals and applications in high performance liquid chromatography, J. Chromatogr. A 1357 (2014) 36–52.

[3] F. Gritti, T. Farkas, J. Heng, G. Guiochon, On the relationship between band broadening and the particle-size distribution of the packing material in liquid chromatography: Theory and practice., J. Chromatogr. A 1218 (2011) 8209–8221.

[4] F. Gritti, G. Guiochon, Mass transfer kinetics, band broadening and column efficiency, J. Chromatogr. A 1221 (2012) 2–40.

[5] M. Catani, O. H. Ismail, A. Cavazzini, A. Ciogli, C. Villani, L. Pasti, D. Cabooter, G. Desmet, F. Gasparrini, D. S. Bell, Rationale behind the optimum efficiency of columns packed gwith the new 1.9 μm fully porous particles Titan c_{18}, J. Chromatogr. A 1454 (2016) 78–85.

[6] R. W. Brice, X. Zhang, L. A. Colón, Fused-core, sub-2 microm packings, and monolithic HPLC columns: a comparative evaluation, J. Sep. Sci. 32 (2009) 2723–2731.

[7] F. Gritti, I. Leonardis, D. Shock, P. Stevenson, A. Shalliker, G. Guiochon, Performance of columns packed with the new shell particles Kinetex-C_{18}, J. Chromatogr. A 1217 (2010) 1589–1603.

[8] A. Cavazzini, L. Pasti, A. Massi, N. Marchetti, F. Dondi, Recent applications in chiral high performance liquid chromatography: A review, Anal. Chim. Acta 706 (2011) 205–222.

[9] R. J. Reischl, L. Hartmanova, M. Carrozzo, M. Huszar, P. Frühauf, W. Lindner, Chemoselective and enantioselective analysis of proteinogenic amino acids utilizing

n-derivatization and 1-d enantioselective anion-exchange chromatography in combination with tandem mass spectrometric detection, J. Chromatogr. A 1218 (2011) 8379–8387.

[10] K. Lomsadze, G. Jibuti, T. Farkas, B. Chankvetadze, Comparative high-performance liquid chromatography enantioseparations on polysaccharide based stationary phases prepared by coating totally porous and core-shell silica particles, J. Chromatogr. A 1234 (2012) 50–55.

[11] S. Fanali, G. D'Orazio, T. Farkas, B. Chankvetadze, Comparative performance of capillary columns made with totally porous and core-shell particles coated with a polysaccharide-based chrial selector in nano-liquid chromatography and capillary electrochromatography, J. Chromatogr. A 1269 (2012) 136–142.

[12] S. Rocchi, S. Fanali, T. Farkas, B. Chankvetadze, Effect of content of chiral selector and pore size of core-shell type silica support on the performance of amylose tris(3,5-dimethylphenylcarbamate)-based chiral stationary phases in nano-liquid chromatography and capillary electrochromatography, J. Chromatogr. A ~~1234 (2012) 50–55~~ 1363 (2014) 363–371.

[13] J. W. Treadway, K. D. Wyndham, J. W. Jorgenson, Highly efficient capillary columns packed with superficially porous particles via sequential column packing, J. Chromatogr. A 1422 (2015) 345–349.

[14] J. P. Grinias and R. T. Kennedy, Evaluation of 5 μm superficially porous particles for capillary and microfluidic LC columns, Chromatography 2 (2015) 502–514.

[15] C. Fanali, A. Rocco, Z. Aturki, L. Mondello, S. Fanali, Analysis of polyphenols and methylxantines in tea samples by means of nano-liquid chromatography utilizing capillary columns packed with core-shell particles, J. Chromatogr. A 1234 (2012) 38–44.

[16] G. D'Orazio, S. Rocchi, S. Fanali, Nano-liquid chromatography coupled with mass spectrometry: Separation of sulfonamides employing non-porous core-shell particles, J. Chromatogr. A 1255 (2012) 277–285.

[17] S. Bruns, D. Stoeckel, B. M. Smarsly, U. Tallarek, Influence of particle properties on the wall region in packed capillaries, J. Chromatogr. A 1268 (2012) 53–63.

[18] L. E. Blue, J. W. Jorgenson, 1.1 μm superficially porous particles for liquid chromatography: Part II: Column packing and chromatographic performance, J. Chromatogr. A 1380 (2015) 71–80.

[19] S. Bruns, E. G. Franklin, J. P. Grinias, J. M. Godinho, J. W. Jorgenson, U. Tallarek, Slurry concentration effects on the bed morphology and separation efficiency of capillaries packed with sub-2 m particles, J. Chromatogr. A 1318 (2013) 189 – 197.

[20] D. C. Patel, Z. S. Breitbach, M. F. Wahab, C. L. Barhate, D. W. Armstrong, Gone in seconds: praxis, performance and peculiarities of ultrafast chiral liquid chromatography with superficially porous particles, Anal. Chem. 87 (2015) 9137–9148.

[21] D. A. Spudeit, M. D. Dolzan, Z. S. Breitbach, W. E. Barber, G. A. Micke, D. W. Armstrong, Superficially porous particles vs. fully porous particles for bonded high performance liquid chromatographic chiral stationary phases: Isopropyl cyclofructan 6, J. Chromatogr. A 1363 (2014) 89–95.

[22] C. L. Barhate, Z. S. Breitbach, E. Costa Pinto, E. L. Regalado, C. J. Welch, D. W. Armstrong, Ultrafast separation of fluorinated and desfluorinated pharmaceuticals using highly efficient and selective chiral selectors bonded to superficially porous particles, J. Chromatogr. A 1426 (2015) 241–247.

[23] A. Cavazzini, N. Marchetti, R. Guzzinati, M. Pierini, A. Ciogli, D. Kotoni, I. D'Acquarica, C. Villani, F. Gasparrini, Enantioseparation by ultra-high-performance liquid chromatography, Trends Anal. Chem. 63 (2014) 95–103.

[24] L. Sciascera, O. Ismail, A. Ciogli, D. Kotoni, A. Cavazzini, L. Botta, T. Szczerba, J. Kocergin, C. Villani, F. Gasparrini, Expanding the potential of chiral chromatography for high-throughput screening of large compound libraries by means of sub-2 μm Whelk-O1 stationary phase in supercritical fluid conditions, J. Chromatogr. A (2015) 160–168.

[25] B. L. W.H. Pirkle, C.J. Welch, Design, synthesis, and evaluation of an improved enantioselective naproxen selector, J. Org. Chem 57 (1992) 3854–3860.

[26] W. H. Pirkle, P. G. Murray, An instance of temperature-dependent elution order of enantiomers from a chiral brush-type HPLC column, J. High Resolut. Chromatogr. 16 (1993) 285–288.

[27] D. Kotoni, A. Ciogli, C. Molinaro, I. D'Acquarica, J. Kocergin, T. Szczerba, H. Ritchie, C. Villani, F. Gasparrini, Introducing enantioselective Ultrahigh-Pressure Liquid Chromatography (eUHPLC): theoretical inspections and ultrafast separations on a new sub-2-μm Whelk-O1 stationary phase, Anal. Chem. 84 (2012) 6805–6813.

[28] D. Kotoni, A. Ciogli, I. D'Acquarica, J. Kocergin, T. Szczerba, H. Ritchie, C. Villani, F. Gasparrini, Enantioselective ultra-high and high performance liquid chromatography: a comparative study of columns based on the Whelk-O1 selector, J. Chromatogr. A 1269 (2012) 226–241.

[29] I. D'Acquarica, D. Kotoni, A. Ciogli, M. Pierini, J. Kocergin, H. Ritchie, C. Villani, F. Gasparrini, The evolution of chiral stationary phases from HPLC to UHPLC, LC/GC Europe 27 (2014) 128–137.

[30] A. Cavazzini, L. Pasti, R. Greco, V. Costa, D. Solera, F. Dondi, N. Marchetti, A. Laganà, F. Gasparrini, Geometric characterization of straight-chain perfluorohexylpropyl adsorbents for high performance liquid chromatography, J. Chromatogr. A 1286 (2013) 47–54.

[31] I. Halász, K. Martin, Pore Size of Solids, Angew. Chem. Int. Ed. Engl 17 (1978) 901–908.

[32] A. Cavazzini, F. Gritti, K. Kaczmarski, N. Marchetti, G. Guiochon, Mass-transfer kinetics in a shell packing material for chromatography, Anal. Chem. 79 (2007) 5972–5979.

[33] U. D. Neue, HPLC Columns: Theory, Technology and Practice, Wiley-VCH, 1997.

[34] J. C. Giddings, Dynamics of Chromatography, Marcel Dekker, New York, 1965.

[35] B. Giner and I. Gascón, A. Villares, P. Cea, C. Lafuente, Densities and viscosities of the binary mixtures of tetrahydrofuran with isomeric chlorobutanes at 298.15K and 303.15K, J. Chem. Eng. Data 51 (2006) 1321–1325.

[36] O. H. Ismail, M. Catani, L. Pasti, A. Cavazzini, A. Ciogli, C. Villani, D. Kotoni, F. Gasparrini, D. S. Bell, Experimental evidence of the kinetic performance achievable with columns packed with the new 1.9 μm fully porous particles Titan c_{18}, J. Chromatogr. A 1454 (2016) 86–92.

[37] M. D. Dolzan, D. A. Spudeit, Z. S. Breitbach, W. E. Barber, G. A. Micke, D. W. Armstrong, Comparison of superficially porous and fully porous silica supports used for a cyclofructan 6 hydrophilic interaction liquid chromatographic stationary phase, J. Chromatogr. A 1365 (2014) 124–130.

[38] I. Quiñones, A. Cavazzini, G. Guiochon, Adsorption equilibria and overloaded band profiles of basic drugs in a reversed-phase system, J. Chromatogr. A 877 (2000) 1–11.

[39] K. Kaczmarski, A. Cavazzini, P. Szabelski, D. Zhou, X. Liu, G. Guiochon, Application of the general rate model and the generalized Maxwell-Stefan equation to the study of the mass transfer kinetics of a pair of enantiomers, J. Chromatogr. A 962 (2002) 57–67.

[40] A. Felinger, A. Cavazzini, F. Dondi, Equivalence of the microscopic and macroscopic models of chromatography: Stochastic-dispersive versus lumped kinetic model, J. Chromatogr. A 1043 (2004) 149–157.

[41] J. P. Foley, Resolution equations for column chromatography, Analyst 116 (1991) 1275–1279.

[42] E. Heftmann (Ed.), Chromatography, 5th edition. Fundamentals and applications of chromatography and related differential migration methods. Part A, Elsevier, 1992, Ch. 1.

[43] F. Gritti, I. Leonardis, J. Abia, G. Guiochon, Physical properties and structure of fine core-shell particles used as packing materials for chromatography: Relationships between particle characteristics and column performance, J. Chromatogr. A 1217 (2010) 3819–3843.

[44] V. Baranau, U. Tallarek, Random-close packing limits for monodisperse and polydisperse hard spheres, Soft Matter 10 (2014) 3826–3841.

[45] F. Gritti, G. Guiochon, Speed-resolution properties of columns packed with new 4.6μm Kinetex-c_{18} core-shell particles, J. Chromatogr. A 1280 (2013) 35–50.

[46] F. Gritti, G. Guiochon, Possible resolution gain in enantioseparations afforded by core-shell particle technology, J. Chromatogr. A 1348 (2014) 87–96.

[47] F. Gritti, G. Guiochon, Mass transfer mechanism in chiral reversed phase liquid chromatography, J. Chromatogr. A 1332 (2014) 35–45.

[48] H. Lin, C. Horváth, Viscous dissipation in packed beds, Chem. Eng. Sci. 36 (1981) 47–55.

[49] C. Horváth, H. J. Lin, Band spreading in liquid chromatography. general plate height equation and a method for the evaluation of the individual plate height contributions, J. Chromatogr. 149 (1978) 43–70.

[50] H. Poppe, J. C. Kraak, J. F. K. Huber, J. H. M. v. Berg, Temperature gradients in HPLC columns due to viscous heat dissipation 14 (1981) 515–523.

[51] F. Gritti, M. Martin, G. Guiochon, Influence of viscous friction heating on the efficiency of columns operated under very high pressures, Anal. Chem. 81 (2009) 3365–3384.

[52] A. de Villiers, H. Lauer, R. Szucs, S. Goodall, P. Sandra, Influence of frictional heating on temperature gradients in ultra-high-pressure liquid chromatography on 2.1 mm i.d. columns, J. Chromatogr. A 1113 (2006) 84–91.

[53] F. Gritti, G. Guiochon, Comparison of heat friction effects in narrow-bore columns packed with core-shell and totally porous particles, Chem. Eng. Sci. 65 (2010) 6310–6319.

~~[45] S. Bruns, E. G. Franklin, J. P. Grinias, J. M. Godinho, J. W. Jorgenson, U. Tallarek, Slurry concentration effects on the bed morphology and separation efficiency of capillaries packed with sub-2 m particles, J. Chromatogr. A 1318 (2013) 189 – 197.~~

[54] A. E. Reising, J. M. Godinho, K. Hormann, J. W. Jorgenson, U. Tallarek, Larger voids in mechanically stable, loose packings of 1.3 μm frictional, cohesive particles: Their reconstruction, statistical analysis, and impact on separation efficiency, J. Chromatogr. A 1436 (2016) 118–132.

~~[47] S. Rocchi, S. Fanali, T. Farkas, B. Chankvetadze, Effect of content of chiral selector and pore size of core-shell type silica support on the performance of amylose tris(3,5-dimethylphenylcarbamate)-based chiral stationary phases in nano-liquid chromatography and capillary electrochromatography, J. Chromatogr. A 1363 (2014) 363–371.~~

[55] E. L. Regalado, A. A. Makarov, R. McClain, M. P. C. J. Welch, Search for improved fluorinated stationary phases for separation of fluorine-containing pharmaceuticals from their desfluoro analogs, J. Chromatogr. A 1380 (2015) 45–54.

[56] S. Thurmann, C. Lotter, J. J. Heiland, B. Chankvetadze, D. Belder, Chip-based high-performance liquid chromatography for high-speed enantioseparations, Anal. Chem 87 (2015) 5598–5576.

***Highlights (for review)**

1) Novel Pirkle-type Whelk-O1 core-shell chiral stationary phase was prepared
2) Difficulty of efficiently packing polar core-shell particles is reported
3) Effect of surface coverage on adsorption-desorption kinetics is pointed out
4) Kinetic characterization of new stationary phase in normal phase mode is described
5) Separation of enantiomers in less than 1 second was achieved

Pirkle-type chiral stationary phase on core-shell and fully porous particles: are superficially porous particles always the better choice towards ultrafast high-performance enantioseparations?

Omar H. Ismail[a], Luisa Pasti[b], Alessia Ciogli[a], Claudio Villani[a], Jelena Kocergin[c], Scott Anderson[c], Francesco Gasparrini[a,*], Alberto Cavazzini[b,**], Martina Catani[b]

[a]*Dept. of Drug Chemistry and Technology, "Sapienza" Università di Roma, P.le A. Moro 5, 00185 Roma, Italy*
[b]*Dept. of Chemistry and Pharmaceutical Sciences, University of Ferrara, via L. Borsari 46, 44121 Ferrara, Italy*
[c]*Regis Technologies, Inc., 8210 Austin Avenue, Morton Grove, IL 60053, USA*

Abstract

Pirkle-type Whelk-O1 chiral stationary phase (CSP) was prepared on 2.6 μm superficially porous particles (SPPs). The chromatographic behavior of columns packed with this new CSP was compared with that of columns packed respectively with 1.8 and 2.5 μm Whelk-O1 fully porous particles (FPPs). In the comparison, both thermodynamic and kinetic aspects were considered. Contrary to initial expectations, chiral columns packed with 2.6 μm SPPs were quasi-comparable to those packed with 2.5 μm FPPs, apparently due to larger contributions to band broadening from both eddy dispersion and, especially for the second eluted enantiomer, adsorption-desorption kinetics. These findings raise the question if SPPs, in spite of the undeniable advantages of their morphology to speed up mass transfer, are always the best choice for high-efficient ultrafast chiral separations. The last part of the work focuses on the use of short columns (10 mm long) and very high flow rates to realize the separation of the enantiomers of *trans*-stilbene oxide (TSO) in normal phase mode in less than one second.

Keywords: Whelk-O1 superficially porous chiral stationary phase; ultrafast

*Corresponding author
**Corresponding author (phone:+39.0532.455331; fax: +39.0532.240709)
Email addresses: francesco.gasparrini@uniroma1.it (Francesco Gasparrini), cvz@unife.it (Alberto Cavazzini)

enantioseparations; mass transfer kinetics; sub-second separation; normal phase mode.

1. Introduction

Last generation superficially-porous particles (SPPs) [1, 2], referred to also as core-shell, fused-core or solid-core particles, are made of a non-porous fused silica core surrounded by a porous shell, whose volume is usually 60-75% of particle volume. In terms of mass transfer, core-shell structure offers some advantages over that of a fully porous particle (FPP) since the contributions to band broadening from both the longitudinal diffusion due to the relaxation of axial gradient concentration along the column (the so called B-term of the van Deemter equation) and the solid-liquid mass transfer resistance due to the diffusion across the particle (C-term of the van Deemter equation) are reduced by the presence of the inaccessible core. In addition, columns packed with C_{18}-SPPs have been demonstrated to be extremely efficient also thanks to the very low eddy diffusion, which comes from flow unevenness in the interstitial zone of the column (A-term of the van Deemter equation) [3–5]. Even though the explanation of the low A-term for columns packed with C_{18} SPPs remains to a large extent unknown, the most accepted hypothesis is that roughness of core-shell particles limits particle slipping after releasing the high pressure employed for the preparation of the packed bed by slurry-packing, therefore reducing radial bed heterogeneity [1, 2]. The reason of the great success of SPPs is that they have provided a reasonable compromise between two opposite tendencies. Indeed, the tendency to improve analytical throughputs by means of columns packed with smaller and smaller particles and reduced dimensions is limited by instrumental factors, such as the extremely high pressures needed to operate these columns at high flow rates, on the one hand, and the effect of system extra-column volume on peak broadening, on the other. As a matter of fact, columns packed with 2.7 μm SPPs are able to provide essentially the same efficiency as columns packed with sub 2-μm FPPs (keeping constant column dimensions and experimental conditions), but at operating pressures similar to those of columns packed with 3 μm FPPs [6, 7].

Surprisingly, the employment of SPPs in chiral chromatography is relatively recent [8]. The first work describing the use of SPPs in chiral HPLC dates 2011, when Lindner and coworkers prepared [9] a cinchona alkaloid based anion exchanger CSP by using 2.7 μm fused-core particles as base material. The column was successfully employed for the enantioseparation of amide type amino acid derivatives, even if the authors do not mention the possible advantages given by this typology of CSP. Chankvetadze and al. [10] firstly compared the kinetic performance of CSPs prepared on polysaccharide-coated FPPs and SPPs. They mentioned some of the benefits of chiral SPPs over their fully porous counterparts, such as an higher enantioselectivity at comparable content of chiral selector, a limited dependence of plate height on mobile phase flow rate and a larger enantioresolution per analysis time, with obvious benefits for high-throughput screening of chiral compounds [10]. By using 4.6 mm I.D.$\times$250 mm columns, they demonstrated that columns packed with SPPs outperform those packed with FPPs in terms of efficiency and speed of analysis. Fanali and coworkers [11, 12] employed the same polysaccharide-based chiral particles used in [10] to pack capillary columns (75μm I.D.$\times$25 cm) for nano-liquid chromatography and electrochromatography experiments. They report about the difficulty to efficiently operate these capillaries. They conclude that, without further optimization, this column format does not allow to reach useful efficiency for high-performance separation. Even if the authors do not discuss in detail the reason of the poor performance of these packed capillaries, more than on the kinetic performance of particles themselves, this could depend either on the difficulty of efficiently packing chiral core-shell particles (and thus to the contribution of eddy dispersion to peak broadening) or on the overall difficulty in getting efficient SPP columns at the capillary scale [13–19].

The most systematic work on the comparison between chiral FPPs and SPPs has been done by Armstrong's group [20–22]. With the aim of investigating the potential of chiral SPPs for ultrafast enantioseparations, Armstrong and coworkers characterized a wide variety of bonded brush-type CSPs prepared on 2.7 μm SPPs, including cyclofructan-6 based, β-cyclodextrin and macrocyclic antibiotics (in particular, teicoplanin, teicoplanin

aglycone and vancomycin) [20]. The concept that emerges from these studies is that chiral SPPs outperform their FPP counterparts in any chromatographic mode, namely, reversed-phase (RP), normal phase (NP), polar organic and HILIC.

In the first part of this paper, we report about the synthesis of novel Pirkle-type Whelk-O1 2.6 μm chiral SPPs and the kinetic characterization of columns packed with these particles. To this scope, a comparison between the performance of these columns and those of columns packed with both 2.5 and 1.8 μm FPPs functionalized with identical chiral selector [23, 24] was performed by using *trans*-stilbene oxide (TSO) enantiomers as probes. In the second part of the work, the potential of Whelk-O1 CSPs for ultrafast enantioseparations on the second/sub-second time-scale is investigated by means of short columns (10 mm packed with both FFPs and SPPs) operated at very high flow rates (up to 8 ml/min).

2. Experimental section

Columns and materials. All solvents and reagents employed in this work were purchased from Sigma-Aldrich (St. Louis, MI, USA). Kromasil silica (1.8 and 2.5 μm particle size, 100 Å pore size, 323 m^2/g specific surface area) was from Akzo-Nobel (Bohus, Sweden). Whelk-O1 selector was generously donated by Regis Technologies Inc (Morton Grove, IL, USA). Accucore silica (2.6 μm particle size, 80 Å pore size, 130 m^2/g specific surface area, 0.5 μm shell thickness) was from Thermo Fisher Scientific (Waltham, MA, USA). 150 and 100 mm$\times$4.6 mm empty stainless steel columns were from IsoBar Systems by Idex (Erlangen, Germany), while 10$\times$4.6 and 10$\times$3.0 mm ones (including their holders) were fully developed and produced in-house. Fourteen polystyrene standards (from Supelco Sigma-Aldrich, Milan, Italy) with molecular weights 500, 2000, 2500, 5000, 9000, 17500, 30000, 50000, 156000, 330000, 565000, 1030000, 1570000, 2310000 were employed for inverse size exclusion chromatography (ISEC).

Equipment. Two chromatographic equipments were employed in this work. Unless differently specified, the UHPLC chromatographic system used for 150 and 100 mm columns was an UltiMate 3000 RS system from Thermo Fisher Dionex (Whaltam, MA, USA) con-

sisting of a dual gradient RS pump (flow rates up to 8.0 mL/min; pressure limit 800 bar under NP conditions), an in-line split loop Well Plate Sampler, a thermostated RS Column Ventilated Compartment and a diode array detector (UV Vanquish) with a low dispersion 2.5 μL flow cell. Detection wavelength was 214 nm (constant filter time: 0.002 s; data collection rate: 100 Hz; response time: 0.04 s). To reduce the extra-column contributions two 350$\times$0.10 mm I.D. Viper capillaries were used to connect the injector to the column and the column to the detector. The extra-column peak variance (calculated through peak moments) was 5.5 μL^2 in Hex/EtOH 90:10 + 1% MeOH at a flow-rate of 1.0 mL/min (extra-column volume: 12.2 μL). Data acquisition, data handling and instrument control were performed by Chromeleon (vers. 6.8) sofware.

An UPLC Acquity Waters system (Milford, MA, USA), equipped with a binary solvent manager (2mL/min maximum flow rate; pressure limit 1000 bar), an auto-sampler with a 5 μL injection loop, a thermostated column compartment (operated in still air conditions [5]), a diode array detector with a 500 nL flow cell, 80 Hz acquisition rate (resolution 4.8 nm; no filter time constant) was employed. Two Viper capillaries (250$\times$0.100 mm and 350$\times$0.100 mm $L\times$I.D.) were used as inlet and outlet connectors. The extra-column peak variance (through peak moments) was only 0.91 μL^2 at 1.0 mL/min. An updated version of Empower software was used in order to measure the second central time moments of the recorded concentration profiles. For the 10 mm columns, a modified version of the UPLC was used (Fig. S1 of Supplementary Data shows some images of the experimental arrangement). The programmable auto-sampler was replaced with an external in-house modified sample injector from VICI, Houston, TX, USA (model C74U). Essentially, this modification allowed for an electronic and fine control of the switching time (1.10 s) from injection to loading position and back. The injector is equipped with a 50 nL internal injection loop and a micro-electric actuator (Valco instruments, Houston, TX, USA). The sample solution was introduced through a 25 μL syringe. This arrangement ensured consistent reduction of tailing effect and high reproducibility between injections. The standard inlet and outlet connecting tubes were replaced by two PEEK tubings of, re-

spectively, 50 and 60 mm length $\times$ 63.5 μm I.D. With this configuration, the extra-column peak variance (through peak moments) was only 0.14 μL^2 at 1.0 mL/min.

Synthesis of Whelk-O1 SPPs and preparation of columns. Whelk-O1 SPPs were synthesized according to the procedure described by Pirkle and co-workers in 1992 [25, 26], which has been also employed for the synthesis of Whelk-O1 FPPs [27–29].

CHN elemental analysis for the different silica types functionalized in this work returned the following values: 6.28% C, 0.84% H and 0.73% N for 2.6 μm SPPs; 13.41% C, 1.73% H and 1.39% N for 1.8 μm FPPs; 13.30% C, 1.73% H and 1.38% N for 2.5 μm FPPs. Calculated bonding densities (based on N) are reported in Table 1. Details on how these calculations were performed can be found in reference [30]. FT-IR (KBr) of Whelk-O1 were: 2924, 2864, 1675, 1627, 1548, 1513, 1344, 1078 cm^{-1}.

All columns were slurry packed with a pneumatically driven Haskel pump (P_{max} = 1000 bar). The slurry solution (10% w/v of Whelk-O1 particles in acetone) was pushed into the column by using a mixture of hexane/2-propanol 90:10 (% v/v) as pushing solvent. The pressure was increased from 400 bar up to 1000 bar. 100 mL of pushing solvent were pumped into the column at 1000 bar to consolidate the bed. Decompression until atmospheric pressure was gradually performed.

van Deemter curve measurements. The kinetic performance of Whelk-O1 columns was evaluated in NP conditions. The mobile phase was a mixture of hexane/ethanol 90:10 (% v/v) + 1% methanol. Injection volumes were 0.1-0.5 μL. Temperature was set at 35°C. Retention time (t_R) and column efficiency (number of theoretical plates, N) of eluted peaks were automatically processed by the Chromeleon and Empower 3 software (using peak width at half height, according to European Pharmacopeia). N values were not corrected by extra-column contribution. The flow rates employed for studying the dependence of height equivalent to a theoretical plate H (=L/N, being L the column length) on the mobile phase velocity started from 0.1 mL/min up to maximum respectively of 4.0 mL/min (for 100 and 150 mm long columns; equipment: Dionex 3000RS) and 2.0 ml/min (for 10 mm long columns; equipment: Waters Acquity), with constant steps of 0.1 mL/min.

van Deemeter curves were plotted as H vs. interstitial velocity, u_{int}. u_{int} was calculated according to the well known equation:

$$u_{int} = \frac{F_v}{\pi r^2 \epsilon_e} \tag{1}$$

being F_v the flow rate, r the radius of the column and ϵ_e the interstial porosity. ϵ_e was calculated by ISEC experiments, as described below.

ISEC measurements, estimation of interstitial and total porosity and retention factor evaluation. ISEC measurements were performed by using tetrahydrofuran as mobile phase [31]. Injection volume, flow rate and detection wavelength were, respectively, 2 μL, 0.1 mL/min and 254 nm. For ISEC plots, retention volumes were corrected for the extra-column contribution before being plotted against the cubic root of the molecular weight (M_W). The interstitial volume, V_e, was derived from the extrapolation to $M_W = 0$ of the linear regression calculated for the volumes of the totally excluded polystyrene samples [32]. From this, the estimation of external column porosity, ϵ_e, is straightforward (being $\epsilon_e = V_e/V_{col}$, with V_{col} the geometric volume of the column). The ISEC estimation of the thermodynamic void volume, V_0, was based on the retention volume of benzene. Through this, the total porosity ϵ_t can be calculated ($\epsilon_t = V_0/V_{col}$).

The retention factor for the i-th enantiomer, k_i, was calculated by:

$$k_i = \frac{t_{R,i} - t_0}{t_0} \tag{2}$$

where $t_{R,i}$ is the retention time of the i-th enantiomer ($i = 1, 2$) and t_0 the void time calculated by using carbon tetrachloride (CCl_4) as marker.

Specific permeability and Kozeny-Carman constant. The specific permeability of each column was calculated according to the traditional equation [33, 34]:

$$k_0 = \frac{u \eta L}{\Delta P} \tag{3}$$

where $u = F_v/\pi r^2$ is the superficial velocity and η the viscosity of the eluent (0.46 cP for THF at 25°C [35]). ΔP is the difference between the total pressure drop, P_{tot}, and

the system pressure drop (without the column), P_{ex}. P_{ex} was measured by replacing the column with a zero-volume connector. Experimentally, k_0 can be estimated by the slope of ΔP vs. u plot [36].

The Kozeny-Carman constant K_c was estimated by [33]:

$$K_c = \frac{\epsilon_e^3}{(1-\epsilon_e)^2}\frac{d_p^2}{k_0} \tag{4}$$

where d_p is the particle size (nominal d_ps given by manufacturer were used in this work in place of the more correct Sauter diameter value [5]).

3. Results and discussion

The preparation of SPPs was performed by following the same experimental protocol described in [27–29] for the functionalization of sub-2μm FPPs. The synthesis is particularly advantageous and reproducible even on SPPs, since phenomena such as particle aggregation and clogging or the non-uniform/excessive selector coating, frequently encountered with other chiral selectors, do not represent an issue with Whelk-O1 selector. Table 1 lists the characteristics of the particles employed in this work in terms of dimension, specific surface area, pore size (data from manufacturers) and chiral-selector loading (see Experimental section). Surface coverage is given both as μmol per gram of bare silica (column 6 of Table 1) and μmol per square meter (column 7). Several things can be observed from this table. The first is that the synthesis of FPPs of different dimensions is extremely reproducible (practically the same loading of chiral selector, about 390 μmol/g or 1.2 μmol/m^2, was found on the 1.8 and 2.5 μm FPPs). The second is that, by keeping constant the experimental conditions, functionalization of bare silica leads to significantly larger surface coverage of chiral selector (+ 20%) on SPPs (1.5 μmol/m^2) than on fully porous ones (1.2 μmol/m^2). This could be due to different reasons such as larger accessibility of external layers of particles, different surface chemistry of base silica FPPs and SPPs, etc. However, it is difficult to generalize these findings. They are indeed consistent with previous reports by Armstrong and coworkers [20, 21], but contrast with other data

from the same group [37]. Obviously, since the specific area per gram of FPPs is larger than that of SPPs, the total amount of chiral selector bounded per gram of base silica is also greater on the former type of particles than on fused-core ones.

The common understanding is that the larger the amount of chiral-selector tethered to the surface, the larger the loadability of the phase (which is definitely important in preparative applications [38–40]) and the larger the retention factor. On the other hand, the relationship between enantioselectivity and surface coverage of chiral selector is not straightforward, since this last could impact also on the adsorption-desorption kinetics and thus on the separation efficiency. The resolution, R_s, of two chromatographic peaks (defined by the peak separation divided by the mean peak width) can be indeed expressed as [41]:

$$R_s = \frac{\sqrt{N}}{2}\frac{\alpha - 1}{\alpha + 1}\frac{\bar{k}}{1 + \bar{k}} \tag{5}$$

where N is the number of theoretical plates, and $\bar{k}$ and α are, respectively, the average retention factor (i.e., the average of retention factors of the two enantiomers) and the selectivity, defined by [42]:

$$\alpha = \frac{k_2}{k_1} \tag{6}$$

According to Eq. 5, one observes that resolution not only depends on the fact that solutes must be retained ($\bar{k} \neq 0$) and that they must be retained at different extent ($\alpha \neq 1$), but also on the efficiency of the column, with higher efficiencies giving better resolution.

Fig. 1 shows the chromatograms recorded for the separation of TSO enantiomers on, respectively, the 150×4.6 mm I.D. column packed with 2.5 μm FPPs (top), the 100×4.6 mm I.D. one packed with 1.8 μm FPPs (middle) and, finally, the 150×4.6 mm I.D. column packed with 2.6 μm SPPs (bottom). On each column, the flow rate (see figure caption) at which the chromatogram was recorded corresponds to the optimal flow rate, that is where the van Deemter curve presents its minimum (see later on). For the sake of comparison between different columns, the x-axis is expressed as retention factor (in place of the traditional retention time). Retention factors were calculated by using CCl_4 as the void volume marker (see the experimental section). As it can be noticed from Fig. 1, on

the two columns packed with 2.5 μm and 1.8 μm FPPs, TSO enantiomers are characterized by the same retention factors ($k_1 = 0.69$ and $k_2 = 1.72$), with α equal to 2.49. On the other hand, on the column packed with 2.6 μm SPPs, retention of both enantiomers is smaller ($k_1 = 0.50$ and $k_2 = 1.27$) but α is slightly larger (2.54). On the same figure the efficiency (N/m) of each peak has also been reported. N was calculated as described in the experimental section. In all cases, very large values were observed. In particular, on the 100×4.6 mm I.D. column packed with 1.8 μm FPPs (middle chromatogram), an efficiency as large as 292,000 and 271,000 N/m was obtained respectively for the first and the second eluted enantiomer. As a marginal remark, it can be observed that these values are typical of efficient RP systems [5, 36]. The resolution of columns, estimated by eq. 5, resulted very large as well. R_s is 19.6 on the column packed with 1.8 μm FPPs, 20.2 for the column packed with 2.5 μm FPPs and 17.3 on the column packed with core-shell particles. Therefore, the column packed with SPPs has the lowest R_s, even if the surface density of chiral-selector measured on these particles was the highest (Table 1). However, the overall much higher surface area for FPPs can outweigh this feature and explain this fact. The difference in R_s between columns packed with FPPs could reflect not only the difference in column length and thus in the total N per column (Fig. S2 of Supplementary Data graphically shows this concept by reporting, for the three columns, N per column as a function of velocity) but also the impact of particle size (1.8 vs. 2.5 μm) on the measured efficiency. On the other hand, to explain the smallest R_s measured on the core-shell column one has to consider that the very favourable contribution of α is ruled out by both the effect of efficiency and retention.

Table 2 reports some of the physico-chemical parameters in use to assess the quality of column packing, at least from a qualitative viewpoint, such as the external porosity, ϵ_e, and the Kozeny-Carman constant (see Eq. 4). For well packed columns, ϵ_e is roughly 0.4 [1, 43] and 0.37 [5, 44] respectively for beds made of core-shell and fully porous particles and the K_c constant is close to 180 [33]. As it can be seen from this table, for all columns ϵ_e was about 40%. However, while the columns packed with FPPs have K_c equal to 180,

for the one packed with SPPs K_c is only 160. For the sake of completeness, in Table 2, the total porosities, ϵ_t, of columns are also reported (see the experimental section for details). Their values are close to typical values for columns packed with fully porous (0.65-0.7) and core-shell (0.52-0.55) particles [32, 39, 45].

The other important information that can be derived from Table 2 is about the permeability (see Eq. 3) of columns. As expected, the column packed with 1.8 μm FPPs is characterized by the smallest k_0 value, 2.95×10^{-11} cm^2, which reflects the difficulty of delivering a flow in a bed made of very fine particles. Surprisingly, the column packed with 2.6 SPPs results to be about 25% more permeable than that packed with 2.5 FPPs, even tough their ϵ_e are very similar. This could suggest a less dense packing of SPPs that, together with the already discussed low value of K_c, could affect the kinetic performance of the column.

When the van Deemter equation is employed in chiral chromatography, in addition to the traditional terms describing longitudinal diffusion (B), eddy dispersion (A) and solid-liquid mass transfer kinetics (C_S), an additional term taking into account the slow adsorption-desorption kinetics (C_{ads}), which frequently characterizes enantiorecognition phenomena, is also added [4, 46]. The dependence of H on the mobile phase velocity is therefore written as:

$$H = A(u) + \frac{B}{u} + C_S u + C_{ads} u \tag{7}$$

Fig. 2 shows the van Deemter curves of TSO enantiomers measured, respectively, on the 150×4.6 mm column packed with 2.5 μm FPPs (top), on the 150×4.6 mm one packed with 2.6 μm SPPs (middle) and on the 100×4.6 mm column packed with 1.8 μm FPPs (bottom). Diamonds (green) refer to the first enantiomer and circles (blue) to the second one. The height equivalent to a theoretical plate has been plotted against the interstitial velocity, u_{int} (Eq. 1), which represents the true linear velocity of the mobile phase (since the fluid flows around and between the particles, not through them). These plots suggest some considerations. First, one may observe that the longitudinal diffusion of the two enantiomers in each column is the same. This is demonstrated by the overlapping of their

van Deemter curves at low flow rates (where the B-term is dominant). Then, under the assumption of the same eddy dispersion for the two enantiomers in a given column [47], the conclusion is reached that the difference in the van Deemter curves (already evident at relatively low linear velocity, starting at u_{int} roughly 0.3 cm/s) is essentially due to a slow adsorption-desorption process. This is particularly evident for the column packed with 2.6 μm SPPs (middle plot). Another interesting observation coming from Fig. 2 is that the slope of the C-branch of the van Deemter equation is markedly steeper for the column packed with 1.8 μm FPPs (bottom part of the figure) than for columns packed with both 2.5μm FPPs (top) and 2.6 μm SPPs (middle). This is due to frictional heating generated by the stream of mobile phase against the packed bed of the column through which it percolates under significant pressure gradient [48–50]. For instance, at u_{int}=0.8 cm/s, the back-pressure generated by the 1.8 μm column was 5300 psi and, at u_{int}=1.0 cm/s, it reached 6750 psi. The heat produced locally is dissipated in both the radial and longitudinal direction of the column. This generates longitudinal and radial temperature gradients, whose amplitude depends on the degree of thermal insulation of the column (either adiabatic or isothermal). The column compartment of the Dionex UHPLC equipment used for the measurement of the van Deemter curves with these columns (see Experimental section) can only work in the so-called forced-air mode (quasi-isothermal conditions), where it is well known that radial temperature gradients degrade the efficiency of column [51–53].

With the purpose of comparing the behavior of the three columns, in Fig. 3 van Deemter curves of the first and the second TSO enantiomer are overlapped. Curves on top of this figure are those for the less retained enantiomer, while on the bottom there are the van Deemter curves relative to the second enantiomer. The kinetic behavior of the first enantiomer looks very similar on all columns, in consequence of the very low retention (see Fig. 1) of this compound that does not allow to draw any significant conclusion on mass transfer phenomena. The only minor difference is around the minimum of van Deemter curves, where the core-shell column is the less efficient (see later on).

By considering the second enantiomer (bottom part of Fig. 3), very different kinetic

behaviors can be observed, depending on column. Unexpectedly, the column packed with Whelk-O1 2.6 μm SPPs (circles, purple), no matter the flow rate, is characterized by the worst performance, even worse than its 2.5 μm fully porous counterpart (diamonds, cyan). This is a surprising result that contrasts with the commonly observed performance of columns packed with C_{18} SPPs [6, 7]. It can be explained by considering the contribution to band broadening coming from either eddy dispersion or slow adsorption-desorption kinetics or a combination of both. The first statement, about the importance of eddy dispersion in columns packed with SPPs, is counter intuitive at least according to literature data that demonstrate how packed beds made of SPPs are expected to be more efficient than those of FPPs (see before). It can be however suggested by the experimental difficulties encountered during the slurry packing of Whelk-O1 SPPs. By considering their characteristics, first of all that these particles are polar, however it does not seem weird that they behave differently from hydrophobic C_{18} ones during the slurry packing [19, 54]. As a matter of fact, not only the achievement of stable slurry suspensions was more difficult with very polar SPPs than with Whelk-O1 fully porous ones but also, e.g., the time needed to compress the bed (by high-pressure flushing) did not follow any expected trend and could not be optimized. In conclusion, the impression is that one of the most important characteristics of hydrophobic core-shell particles, i.e. their ability to generate very efficient packed beds, could not be easily reproducible with very polar Whelk-O1 SPPs. Further investigation is needed to assess this point, in particular on rheological characteristics of Whelk-O1 SPPs. In agreement with [11, 12], it should be concluded that the efficient preparation of packed beds of polar SPPs still requires a long way to go. This essentially needs the optimization of all steps of packing protocol, without which the full potential of polar chiral SPPs can be barely reached.

As mentioned before, on the 2.6 μm Whelk-O1 core-shell column the contribution to band broadening coming from a slow mass transfer process seems to be particularly evident. Since the solid-liquid mass transfer term (C_s) should be lower on core-shell than on fully porous particles (due to the presence of the inaccessible core), the conclusion

is that the adsorption-desorption kinetics must be slower on core-shell particles (higher C_{ads} term in eq. 7) than on the fully porous ones. An explanation could be the different surface density of chiral selector between core-shell and FPPs. Table 1 shows that this surface density is about 20% larger on SPPs than on fully porous ones. In literature there are practically no studies which have attempted to assess if and how chiral recognition is modified by changing the amount of chiral selector tethered to the surface and how this could impact on the chromatographic performance [12]. On the other hand, this is a very important subject that needs more experimental and theoretical work to be fully understood.

Finally, by still looking at the bottom part of Fig. 3, it is evident that the column packed with 1.8 μm FPPs (triangles, green) outperform the other two in terms of kinetic behavior but it is also clear that, at high flow rates, where the effect of frictional heating on efficiency is dominant, this column does not offer any advantage over the one packed with 2.5 μm FPPs. Indeed, at u_{int} slightly larger than 1 cm/s, the *C*-branch of the 1.8 μm fully porous column merges to that of the column packed with 2.5 μm FPPs.

Fig. 4 (top) shows the gain in analysis time that can be obtained by moving from both the columns packed with 2.5 μm FPPs and 2.6 μm SPPs to that packed with 1.8 μm FPPs. The necessary premise to discuss this figure – whose meaning is merely practical – is that the length of commercially available columns packed with 2.5-2.7 μm particles (no matter if fully porous or pellicular) is usually 150 mm, while that of columns packed with sub-2μm particles is only 100 mm or less. This justifies the direct comparison presented in Fig. 4, where column length is not accounted for. Having acknowledged this, and by referring for each column to condition of maximum efficiency (indeed chromatograms presented in Fig. 4 were recorded at the optimum flow rate, see figure caption for details), one observes that the column packed with 1.8 μm FPPs permits to decrease analysis time (here simply calculated as the retention time of the second eluted enantiomer) more than 50 and 30% with respect to the 2.5 μm fully porous column and the 2.6 μm core-shell one. The practical advantage achievable with the 100 mm column packed with sub-2μm

particles, becomes still more evident by considering, in addition to analysis time, also the resolution of columns (see before). Thus, the ratio between resolution and analysis time [55], graphically given as bar chart in the bottom part of Fig. 4, is strongly favorable for the 1.8 μm column packed with FPPs (it is indeed 11.9 on this column vs. 5.3 and 7.9 on, respectively, the 2.5 μm fully porous and the 2.6 μm core-shell column). Incidentally, the gain of $R_s/t_{R,2}$ ratio observed for the 2.6 μm core-shell column over that packed with 2.5 μm FPPs comes from the reduction of retention time in the former column (due to a much lower total surface area per column) and not from an increase of R_s (which actually is larger on the 2.5 μm fully porous column).

The last part of this study briefly reports on the use of short columns, packed with both Whelk-O1 FPPs and SPPs, to realize ultrafast enantioseparations. In this proof-of-concept study, 10 mm columns of different I.D. (3.0 and 4.6 mm) were employed. These columns were in-house designed and developed. Fig. S3 of Supplementary Data shows a picture of the 10 mm column and holder. They were packed by following the same protocol also used for longer columns. Table 3 has some information that helps to characterize these columns, in particular the optimal flow rate (i.e., the flow rate corresponding to the minimum of van Deemter curve), the corresponding interstitial linear velocity and the maximum efficiency (in N/m). With the purpose of performing ultrafast enantioseparations, these columns were operated at the maximum flow achievable by instrumentation (8 ml/min). Accordingly, the Thermo Dionex equipment (see experimental section) was employed, even though its extra-column variance is not negligible with respect to that of first and second eluted enantiomers (respectively, roughly 11.2 and 28 μL^2). In the last column of Table 3, the number of theoretical plates per column measured at the highest flow rate is reported. As an example, Fig. 5 shows the chromatogram recorded with the 10$\times$3.0 mm column packed with 1.8 μm FPPs. As it can be seen, the separation of TSO enantiomers was performed in less than 1 s, with $R_s = 2.2$. This represents an extraordinary result, unimaginable only a few years ago in chiral liquid chromatography, which is even comparable with that of chiral separations on microchip platforms [56].

4. Conclusions

The investigation of the kinetic performance of columns packed with Whelk-O1 fully porous and core-shell particles of similar diameter (2.5 μm for FPPs vs. 2.6 μm for core-shell ones) has surprisingly revealed that FPPs outperform SPPs. This depends, in part, on the faster mass-transfer adsorption-desorption kinetics observed (especially on the second eluted enantiomer) on the FPPs and, in part, on the smaller eddy dispersion contribution to band broadening on the column packed with FPPs. The slower mass-transfer adsorption-desorption process is most likely due to the larger surface density of chiral selector on the SPPs. Indeed, even though the same experimental conditions were maintained during functionalization of SPPs and FPPs, the outcome was different. The surface density of Whelk-O1 selector on SPPs was indeed 20% larger than that of FPPs. These results suggest that, at least for the case considered in this work, the higher the surface coverage, the lower the adsorption-desorption process but with the information in our possession no generalization can be made. Fundamental studies aimed at investigating the relationship between mass transfer kinetics and surface density of chiral selector are needed.

On the other hand, the empirical difficulty to pack Whelk-O1 core-shell particles explains the important eddy dispersion contribution to band broadening in columns packed with these particles. Different attempts have been done to improve the packing process, by varying many experimental variables (slurry composition, consolidation time, etc.) during the packing, but without success. These findings show that packing polar SPPs is significantly different from packing hydrophobic SPPs (such as C_{18} particles), for which a large amount of information and expertise has been collected over the years. One of the most significant characteristics of beds made of C_{18} core-shell particles is their extremely low eddy dispersion term. This, however, seems to be difficult to achieve with Whelk-O1 SPPs. The investigation of rheological properties of these particles can help to understand their different behavior with respect to fully porous particles so to optimize the packing protocol and, thus, the kinetic performance of columns made of polar Whelk-O1 SPPs.

5. Acknowledgments

The authors thank the Italian University and Scientific Research Ministry (Grant PRIN 2012ATMNJ_003) and the Laboratory Terra&Acqua Tech, member of Energy and Environment Cluster, Technopole of Ferrara of Emilia-Romagna High Technology Network. Dr. Valentina Costa from the University of Ferrara is acknowledged for technical support. The authors thank Thermo Fisher for providing Accucore 2.6 μm SPP silica.

Appendix A. Supplementary Data

Supplementary data associated with this article can be found in the online version.

6. Figures and Tables

Figure captions

Fig 1. Chromatograms showing the separation of TSO enantiomers on the three columns employed in this work. Carbon tetrachloride was used as dead time marker. Top: 150×4.6 mm column packed with Whelk-O1 2.5 μm FPPs; middle: 100×4.6 mm column packed with Whelk-O1 1.8 μm FPPs; bottom: 150×4.6 mm column packed with Whelk-O1 2.6 μm SPPs. Chromatograms were recorded at the flow rate corresponding to the minimum of the van Deemter curve (they were, from top to bottom, respectively 1.2, 1.8 and 1.5 ml/min). For the sake of comparison, x-axis is given in terms of retention factor instead of retention time. Close to each peak, efficiency (N/m), retention factor (k) and retention time (t_R) are indicated. Instrument employed for measurements: UPLC Waters Acquity.

Fig 2. van Deemter curves for TSO enantiomers measured on Whelk-O1 columns (same geometries as in Fig. 1) packed with, respectively, 2.5 μm FPPs (top), 2.6 μm SPPs (middle) and 1.8 μm FPPs (bottom). Instrument employed for measurements: Dionex 3000RS.

Fig 3. Overlapped van Deemter curves measured on the three Whelk-O1 columns (same geometries as in Fig. 1), respectively for the first (top) and the secondly (bottom) eluted TSO enantiomers. Diamonds: column packed with 2.5 μm FPPs; circles: column packed with 2.6 μm SPPs; triangles: column packed with 1.8 μm FPPs. Instrument employed for measurements: Dionex 3000RS. See text for details.

Fig 4. A) Same chromatograms as in Fig. 1, showing the separation of TSO enantiomers on the three columns employed in this work, but with the x-axis given in retention time. Carbon tetrachloride was used as dead time marker. B) Bar chart showing the ratio between resolution and retention time for the 2.6 μm core-shell column (first bar on the left, blue color), the 1.8 μm fully porous column (middle bar, orange) and, finally, the 2.5 μm

fully porous column (last bar on the right, red). Ratios were calculated on the second eluted enantiomer. Instrument employed for measurements: UPLC Waters Acquity.

Fig 5. Example of ultrafast enantioseparation thanks to the use of short column and high flow rate. In this particular case, a 10×3.0 mm column packed with 1.8 μm FPPs was operated at 8 ml/min (u_{int} = 4.8 cm/s) for the separation of TSO enantiomers. Carbon tetrachloride was used as dead time marker. Note the time scale in seconds. Instrument employed for measurements: Dionex 3000RS. See text for details.

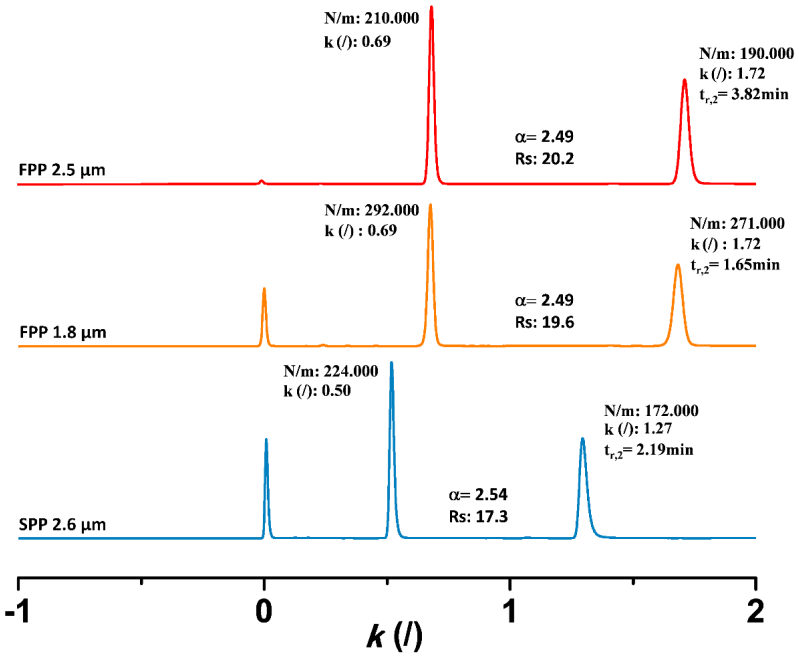

Figure 1:

Figure 1:

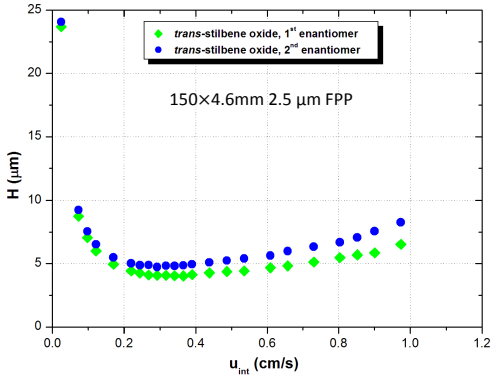
trans-stilbene oxide, 1st enantiomer
trans-stilbene oxide, 2nd enantiomer
150×4.6mm 2.5 µm FPP
H (µm)
u_int (cm/s)

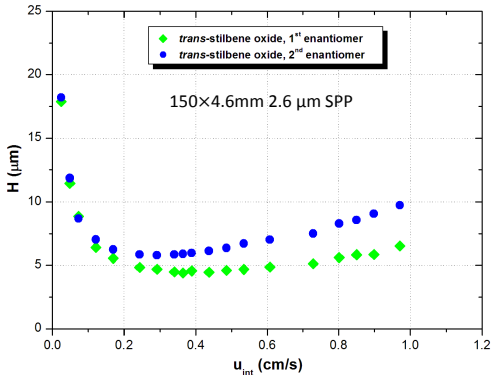
trans-stilbene oxide, 1st enantiomer
trans-stilbene oxide, 2nd enantiomer
150×4.6mm 2.6 µm SPP
H (µm)
u_int (cm/s)

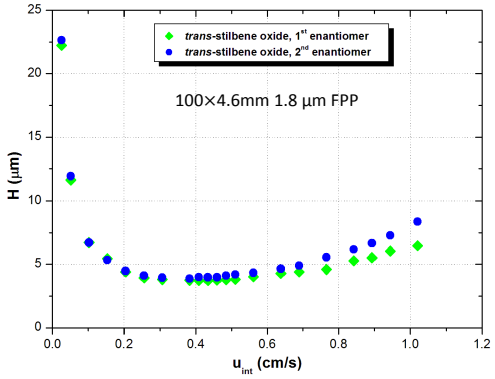
trans-stilbene oxide, 1st enantiomer
trans-stilbene oxide, 2nd enantiomer
100×4.6mm 1.8 µm FPP
H (µm)
u_int (cm/s)

Figure 2:

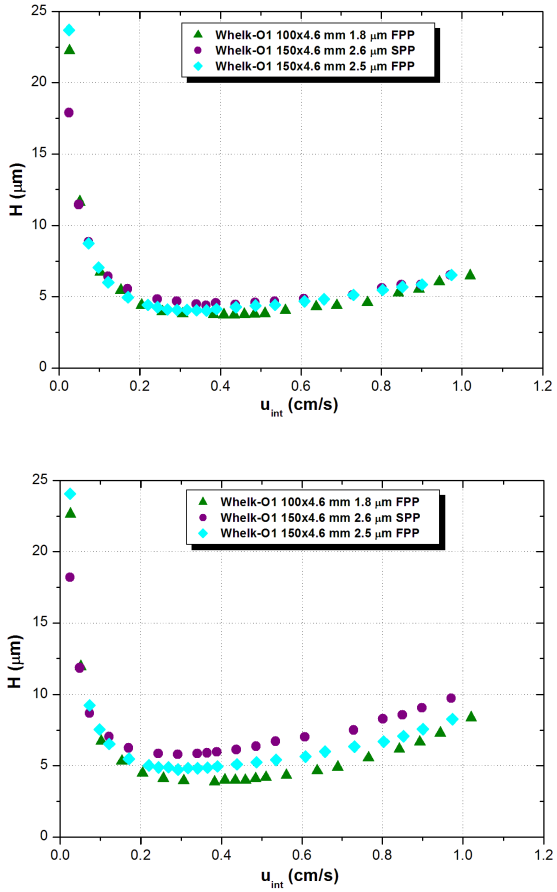
Whelk-O1 100x4.6 mm 1.8 µm FPP
Whelk-O1 150x4.6 mm 2.6 µm SPP
Whelk-O1 150x4.6 mm 2.5 µm FPP
H (µm)
u_int (cm/s)
0
5
10
15
20
25
0.0
0.2
0.4
0.6
0.8
1.0
1.2

Figure 3:

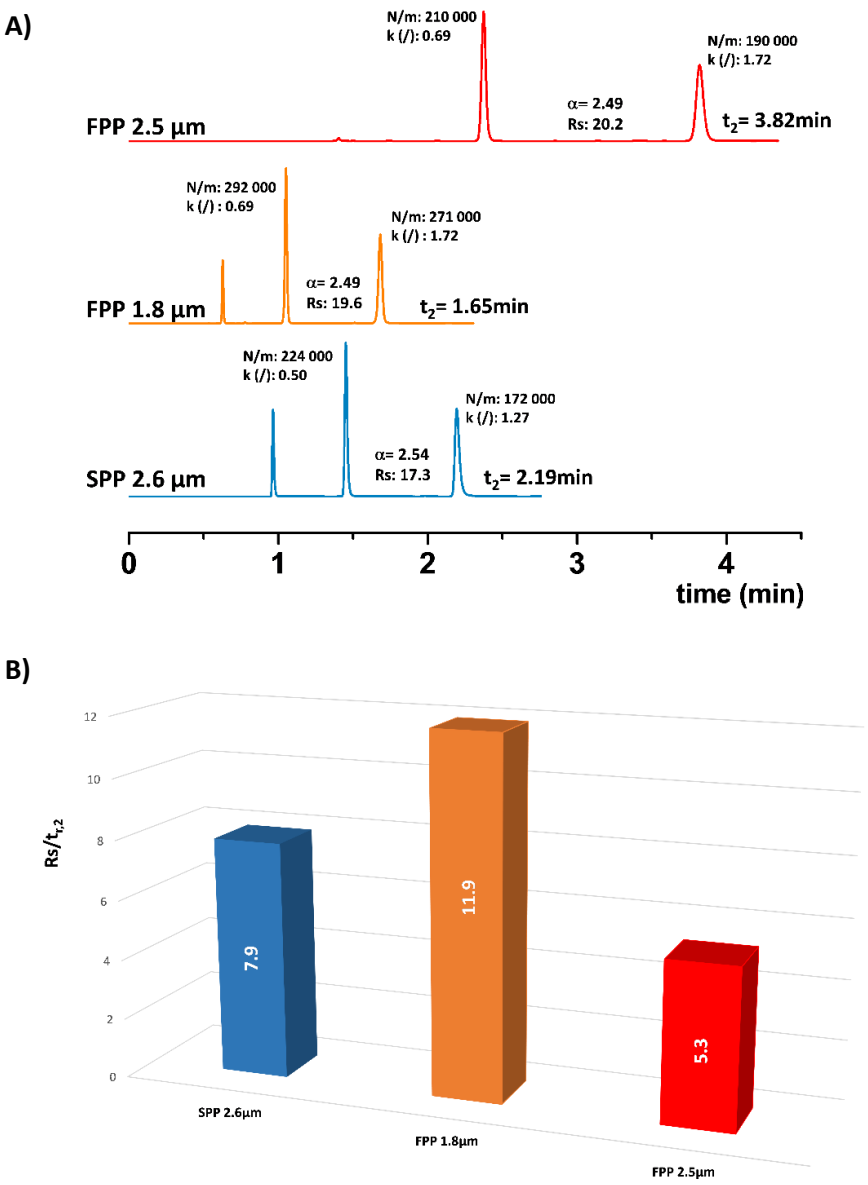
A)
N/m: 210 000
k (/): 0.69
N/m: 190 000
k (/): 1.72
α= 2.49
Rs: 20.2
FPP 2.5 µm
t2= 3.82min
N/m: 292 000
k (/) : 0.69
N/m: 271 000
k (/) : 1.72
α= 2.49
Rs: 19.6
FPP 1.8 µm
t2= 1.65min
N/m: 224 000
k (/): 0.50
N/m: 172 000
k (/): 1.27
α= 2.54
Rs: 17.3
SPP 2.6 µm
t2= 2.19min
0
1
2
3
4
time (min)
B)
Rs/t1,2
12
10
8
6
4
2
0
7.9
11.9
5.3
SPP 2.6µm
FPP 1.8µm
FPP 2.5µm

Figure 4:

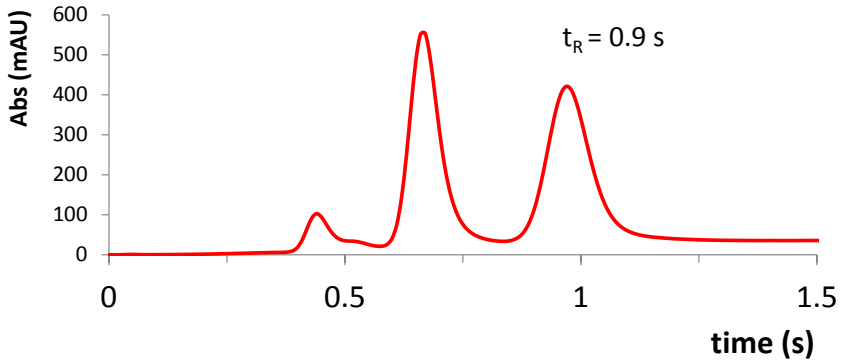

Figure 5:

Table 1: Geometrical characteristics of Whelk-O1 columns: particle type (FP: fully porous, SP: superficially porous); column dimensions; particle diameter (d_p); specific surface area (A_s); pore size; bonding density (given both as μmol per gram of bare silica and μmol per square meter).

Particle type	Dimensions	d_p	A_s	Pore size	Bonding density	
	(L×I.D., mm)	(μm)	(m^2/g)	(Å)	(μmol/g)	(μmol/m^2)
FP	150×4.6	2.5	323	100	391.2	1.21
FP	100×4.6	1.8	323	100	394.6	1.22
SP	150×4.6	2.6	130	80	189.8	1.46

Table 2: Physico-chemical properties of Whelk-O1 columns: particle type (FP: fully porous, SP: superficially porous); total porosity (ϵ_t); external porosity (ϵ_e); Kozeny-Carman constant (K_c); permeability (k_0).

Particle type	ϵ_t	ϵ_e	K_c	$k_0 \times 10^{11}$ (cm^2)
FP	0.670	0.412	180	7.06
FP	0.644	0.393	180	2.95
SP	0.524	0.413	160	8.60

Table 3: Kinetic performance (in N/m) of short columns (10 mm) of different diameter. $F_{v,opt}$ and $u_{int,opt}$ represent, respectively, the optimum flow rate (that is the flow rate corresponding to the minimum of the van Deemter curve) and the optimum interstial velocity; N_{max} is the number of theoretical plates per column, when the column was operated at 8 ml/min (see text for more details). In all cases, N has been calculated as the average value of Ns of the two TSO enantiomers. Particle type: FP, fully porous; SP, superficially porous). Instruments employed for measurements: UPLC Waters Acquity for van Deemter curves; Dionex 3000RS for ultrafast enantioseparations (evaluation of N_{max}).

Particle type	L×I.D. (mm)	$F_{v,opt}$ (mL/min)	$u_{int,opt}$ (cm/s)	N/m	N_{max}
FP	10×4.6	1.7	0.43	190,000	1220
SP	10×4.6	1.5	0.36	140,000	850
FP	10×3.0	0.7	0.42	180,000	520

References

[1] G. Guiochon, F. Gritti, Shell particles, trials, tribulations and triumphs, J. Chromatogr. A 1218 (2011) 1915–1938.

[2] R. Hayes, A. Ahmed, T. Edge, H. Zhang, Core-shell particles: preparation, fundamentals and applications in high performance liquid chromatography, J. Chromatogr. A 1357 (2014) 36–52.

[3] F. Gritti, T. Farkas, J. Heng, G. Guiochon, On the relationship between band broadening and the particle-size distribution of the packing material in liquid chromatography: Theory and practice., J. Chromatogr. A 1218 (2011) 8209–8221.

[4] F. Gritti, G. Guiochon, Mass transfer kinetics, band broadening and column efficiency, J. Chromatogr. A 1221 (2012) 2–40.

[5] M. Catani, O. H. Ismail, A. Cavazzini, A. Ciogli, C. Villani, L. Pasti, D. Cabooter, G. Desmet, F. Gasparrini, D. S. Bell, Rationale behind the optimum efficiency of columns packed gwith the new 1.9 μm fully porous particles Titan c_{18}, J. Chromatogr. A 1454 (2016) 78–85.

[6] R. W. Brice, X. Zhang, L. A. Colón, Fused-core, sub-2 microm packings, and monolithic HPLC columns: a comparative evaluation, J. Sep. Sci. 32 (2009) 2723–2731.

[7] F. Gritti, I. Leonardis, D. Shock, P. Stevenson, A. Shalliker, G. Guiochon, Performance of columns packed with the new shell particles Kinetex-C_{18}, J. Chromatogr. A 1217 (2010) 1589–1603.

[8] A. Cavazzini, L. Pasti, A. Massi, N. Marchetti, F. Dondi, Recent applications in chiral high performance liquid chromatography: A review, Anal. Chim. Acta 706 (2011) 205–222.

[9] R. J. Reischl, L. Hartmanova, M. Carrozzo, M. Huszar, P. Frühauf, W. Lindner, Chemoselective and enantioselective analysis of proteinogenic amino acids utilizing

480 n-derivatization and 1-d enantioselective anion-exchange chromatography in com-
481 bination with tandem mass spectrometric detection, J. Chromatogr. A 1218 (2011)
482 8379–8387.

483 [10] K. Lomsadze, G. Jibuti, T. Farkas, B. Chankvetadze, Comparative high-performance
484 liquid chromatography enantioseparations on polysaccharide based stationary
485 phases prepared by coating totally porous and core-shell silica particles, J. Chro-
486 matogr. A 1234 (2012) 50–55.

487 [11] S. Fanali, G. D'Orazio, T. Farkas, B. Chankvetadze, Comparative performance of
488 capillary columns made with totally porous and core-shell particles coated with a
489 polysaccharide-based chrial selector in nano-liquid chromatography and capillary
490 electrochromatography, J. Chromatogr. A 1269 (2012) 136–142.

491 [12] S. Rocchi, S. Fanali, T. Farkas, B. Chankvetadze, Effect of content of chiral selec-
492 tor and pore size of core-shell type silica support on the performance of amylose
493 tris(3,5-dimethylphenylcarbamate)-based chiral stationary phases in nano-liquid
494 chromatography and capillary electrochromatography, J. Chromatogr. A 1363 (2014)
495 363–371.

496 [13] J. W. Treadway, K. D. Wyndham, J. W. Jorgenson, Highly efficient capillary columns
497 packed with superficially porous particles via sequential column packing, J. Chro-
498 matogr. A 1422 (2015) 345–349.

499 [14] J. P. Grinias and R. T. Kennedy, Evaluation of 5 μm superficially porous particles for
500 capillary and microfluidic LC columns, Chromatography 2 (2015) 502–514.

501 [15] Z. Aturki, L. Mondello, S. Fanali, Analysis of polyphenols and methylxantines in
502 tea samples by means of nano-liquid chromatography utilizing capillary columns
503 packed with core-shell particles, J. Chromatogr. A 1234 (2012) 38–44.

504 [16] G. D'Orazio, S. Rocchi, S. Fanali, Nano-liquid chromatography coupled with mass

spectrometry: Separation of sulfonamides employing non-porous core-shell particles, J. Chromatogr. A 1255 (2012) 277–285.

[17] S. Bruns, D. Stoeckel, B. M. Smarsly, U. Tallarek, Influence of particle properties on the wall region in packed capillaries, J. Chromatogr. A 1268 (2012) 53–63.

[18] J. W. Jorgenson, 1.1 μm superficially porous particles for liquid chromatography: Part II: Column packing and chromatographic performance, J. Chromatogr. A 1380 (2015) 71–80.

[19] S. Bruns, E. G. Franklin, J. P. Grinias, J. M. Godinho, J. W. Jorgenson, U. Tallarek, Slurry concentration effects on the bed morphology and separation efficiency of capillaries packed with sub-2 m particles, J. Chromatogr. A 1318 (2013) 189 – 197.

[20] D. C. Patel, Z. S. Breitbach, M. F. Wahab, C. L. Barhate, D. W. Armstrong, Gone in seconds: praxis, performance and peculiarities of ultrafast chiral liquid chromatography with superficially porous particles, Anal. Chem. 87 (2015) 9137–9148.

[21] D. A. Spudeit, M. D. Dolzan, Z. S. Breitbach, W. E. Barber, G. A. Micke, D. W. Armstrong, Superficially porous particles vs. fully porous particles for bonded high performance liquid chromatographic chiral stationary phases: Isopropyl cyclofructan 6, J. Chromatogr. A 1363 (2014) 89–95.

[22] C. L. Barhate, Z. S. Breitbach, E. Costa Pinto, E. L. Regalado, C. J. Welch, D. W. Armstrong, Ultrafast separation of fluorinated and desfluorinated pharmaceuticals using highly efficient and selective chiral selectors bonded to superficially porous particles, J. Chromatogr. A 1426 (2015) 241–247.

[23] A. Cavazzini, N. Marchetti, R. Guzzinati, M. Pierini, A. Ciogli, D. Kotoni, I. D'Acquarica, C. Villani, F. Gasparrini, Enantioseparation by ultra-high-performance liquid chromatography, Trends Anal. Chem. 63 (2014) 95–103.

[24] L. Sciascera, O. Ismail, A. Ciogli, D. Kotoni, A. Cavazzini, L. Botta, T. Szczerba, J. Kocergin, C. Villani, F. Gasparrini, Expanding the potential of chiral chromatography for high-throughput screening of large compound libraries by means of sub-2 μm Whelk-O1 stationary phase in supercritical fluid conditions, J. Chromatogr. A (2015) 160–168.

[25] B. L. W.H. Pirkle, C.J. Welch, Design, synthesis, and evaluation of an improved enantioselective naproxen selector, J. Org. Chem 57 (1992) 3854–3860.

[26] W. H. Pirkle, P. G. Murray, An instance of temperature-dependent elution order of enantiomers from a chiral brush-type HPLC column, J. High Resolut. Chromatogr. 16 (1993) 285–288.

[27] D. Kotoni, A. Ciogli, C. Molinaro, I. D'Acquarica, J. Kocergin, T. Szczerba, H. Ritchie, C. Villani, F. Gasparrini, Introducing enantioselective Ultrahigh-Pressure Liquid Chromatography (eUHPLC): theoretical inspections and ultrafast separations on a new sub-2-μm Whelk-O1 stationary phase, Anal. Chem. 84 (2012) 6805–6813.

[28] D. Kotoni, A. Ciogli, I. D'Acquarica, J. Kocergin, T. Szczerba, H. Ritchie, C. Villani, F. Gasparrini, Enantioselective ultra-high and high performance liquid chromatography: a comparative study of columns based on the Whelk-O1 selector, J. Chromatogr. A 1269 (2012) 226–241.

[29] I. D'Acquarica, D. Kotoni, A. Ciogli, M. Pierini, J. Kocergin, H. Ritchie, C. Villani, F. Gasparrini, The evolution of chiral stationary phases from HPLC to UHPLC, LC/GC Europe 27 (2014) 128–137.

[30] A. Cavazzini, L. Pasti, R. Greco, V. Costa, D. Solera, F. Dondi, N. Marchetti, A. Laganà, F. Gasparrini, Geometric characterization of straight-chain perfluorohexylpropyl adsorbents for high performance liquid chromatography, J. Chromatogr. A 1286 (2013) 47–54.

[31] I. Halász, K. Martin, Pore Size of Solids, Angew. Chem. Int. Ed. Engl 17 (1978) 901–908.

[32] A. Cavazzini, F. Gritti, K. Kaczmarski, N. Marchetti, G. Guiochon, Mass-transfer kinetics in a shell packing material for chromatography, Anal. Chem. 79 (2007) 5972–5979.

[33] U. D. Neue, HPLC Columns: Theory, Technology and Practice, Wiley-VCH, 1997.

[34] J. C. Giddings, Dynamics of Chromatography, Marcel Dekker, New York, 1965.

[35] A. Villares, P. Cea, C. Lafuente, Densities and viscosities of the binary mixtures of tetrahydrofuran with isomeric chlorobutanes at 298.15K and 303.15K, J. Chem. Eng. Data 51 (2006) 1321–1325.

[36] O. H. Ismail, M. Catani, L. Pasti, A. Cavazzini, A. Ciogli, C. Villani, D. Kotoni, F. Gasparrini, D. S. Bell, Experimental evidence of the kinetic performance achievable with columns packed with the new 1.9 μm fully porous particles Titan c_{18}, J. Chromatogr. A 1454 (2016) 86–92.

[37] 10.1016/j.chroma.2014...etc M. D. Dolzan, D. A. Spudeit, Z. S. Breitbach, W. E. Barber, G. A. Micke, D. W. Armstrong, Comparison of superficially porous and fully porous silica supports used for a cyclofructan 6 hydrophilic interaction liquid chromatographic stationary phase, J. Chromatogr. A 1365 (2014) 124–130.

[38] I. Quiñones, A. Cavazzini, G. Guiochon, Adsorption equilibria and overloaded band profiles of basic drugs in a reversed-phase system, J. Chromatogr. A 877 (2000) 1–11.

[39] K. Kaczmarski, A. Cavazzini, P. Szabelski, D. Zhou, X. Liu, G. Guiochon, Application of the general rate model and the generalized Maxwell-Stefan equation to the study of the mass transfer kinetics of a pair of enantiomers, J. Chromatogr. A 962 (2002) 57–67.

[40] A. Felinger, A. Cavazzini, F. Dondi, Equivalence of the microscopic and macroscopic models of chromatography: Stochastic-dispersive versus lumped kinetic model, J. Chromatogr. A 1043 (2004) 149–157.

[41] J. P. Foley, Resolution equations for column chromatography, Analyst 116 (1991) 1275–1279.

[42] E. Heftmann (Ed.), Chromatography, 5th edition. Fundamentals and applications of chromatography and related differential migration methods. Part A, Elsevier, 1992, Ch. 1.

[43] F. Gritti, I. Leonardis, J. Abia, G. Guiochon, Physical properties and structure of fine core-shell particles used as packing materials for chromatography: Relationships between particle characteristics and column performance, J. Chromatogr. A 1217 (2010) 3819–3843.

[44] V. Baranau, U. Tallarek, Random-close packing limits for monodisperse and polydisperse hard spheres, Soft Matter 10 (2014) 3826–3841.

[45] F. Gritti, G. Guiochon, Speed-resolution properties of columns packed with new 4.6μm Kinetex-c_{18} core-shell particles, J. Chromatogr. A 1280 (2013) 35–50.

[46] F. Gritti, G. Guiochon, Possible resolution gain in enantioseparations afforded by core-shell particle technology, J. Chromatogr. A 1348 (2014) 87–96.

[47] F. Gritti, G. Guiochon, Mass transfer mechanism in chiral reversed phase liquid chromatography, J. Chromatogr. A 1332 (2014) 35–45.

[48] H. Lin, C. Horváth, Viscous dissipation in packed beds, Chem. Eng. Sci. 36 (1981) 47–55.

[49] C. Horváth, H. J. Lin, Band spreading in liquid chromatography. general plate height equation and a method for the evaluation of the individual plate height contributions, J. Chromatogr. 149 (1978) 43–70.

[50] H. Poppe, J. C. Kraak, J. F. K. Huber, J. H. M. v. Berg, Temperature gradients in HPLC columns due to viscous heat dissipation 14 (1981) 515–523.

[51] F. Gritti, M. Martin, G. Guiochon, Influence of viscous friction heating on the efficiency of columns operated under very high pressures, Anal. Chem. 81 (2009) 3365–3384.

[52] A. de Villiers, H. Lauer, R. Szucs, S. Goodall, P. Sandra, Influence of frictional heating on temperature gradients in ultra-high-pressure liquid chromatography on 2.1 mm i.d. columns, J. Chromatogr. A 1113 (2006) 84–91.

[53] F. Gritti, G. Guiochon, Comparison of heat friction effects in narrow-bore columns packed with core-shell and totally porous particles, Chem. Eng. Sci. 65 (2010) 6310–6319.

[54] A. E. Reising, J. M. Godinho, K. Hormann, J. W. Jorgenson, U. Tallarek, Larger voids in mechanically stable, loose packings of 1.3 μm frictional, cohesive particles: Their reconstruction, statistical analysis, and impact on separation efficiency, J. Chromatogr. A 1436 (2016) 118–132.

[55] E. L. Regalado, A. A. Makarov, R. McClain, M. P. C. J. Welch, Search for improved fluorinated stationary phases for separation of fluorine-containing pharmaceuticals from their desfluoro analogs, J. Chromatogr. A 1380 (2015) 45–54.

[56] 10.1021/acs.analchem.5b...etc S. Thurmann, C. Lotter, J. J. Heiland, B. Chankvetadze, D. Belder, Chip-based high-performance liquid chromatography for high-speed enantioseparations, Anal. Chem 87 (2015) 5598–5576.

Electronic Supplementary Material (online publication only)

Click here to download Electronic Supplementary Material (online publication only): suppl_data.pdf

LaTeX Source Files

Click here to download LaTeX Source Files: paper-revised.zip